Macromolecular Materials and Engineering
Open Access
www.mame-journal.de

Graphene Applications in Composites, Energy, and Water Treatment

Maryam A. Saeed, Amor Abdelkader, Yousef Alshammari, Cristina Valles, and Abdullah Alkandary*

Graphene, the 2D material and the basic building block of the sp_2 carbon family has received enormous attention from research and industrial communities due to its remarkable properties. Graphene's potential to be implemented is limitless and it varies from medical, water, energy, composites sectors, etc. In this paper, graphene potential in composites, energy storage, and water purification are highlighted. Reviewing, in particular, the crucial role of graphene/polymer interface in improving the mechanical properties of polymer nanocomposites and the effect of constitutive parameters such as graphene lateral size and surface chemistry. Moreover, the latest contributions of graphene and graphene derivatives in functional composites, such as sensors, actuators, hydrogels, and aerogels, are reviewed. This is followed by reviewing graphene and its derivatives for energy storage such as in lithium-ion batteries, metal–air batteries, and graphene-based supercapacitors. Finally, reporting the latest advances in graphene for water treatment, reviewing the different filtration/treatment methods, and the importance of graphene selective permeability properties.

1. Introduction

Graphene is a single layer of carbon atoms arranged in a 2D honeycomb lattice and it is the basic building block of graphitic materials where a stack of graphene layers form graphite, a rolled graphene sheet forms carbon nanotube and a spherical net forms fullerene. However, among its allotropes, graphene exhibits the most unique and extraordinary properties due to its packed atomic structure with an interatomic distance of 1.42 Å and extremely strong π bonds.[1] Therefore, graphene's unique atomic structure led to its remarkable physical,[2] chemical, electrical, and thermal properties[3] which made graphene a revolutionary material. Since its isolation in 2004, graphene has gained increased interest in both research and industrial sectors, offering potential applications in electronics, energy storage, water treatment, reinforced materials, etc. Its exceptional strength, flexibility, thermal conductivity, and electrical conductivity make it an ideal candidate for implementation in limitless applications.

In electronics, graphene's high electrical conductivity and transparency have paved the way for its use in developing faster, more efficient electronic devices. It is being explored for use in transistors, which could surpass the performance of current silicon-based devices, potentially leading to computers and smartphones that are faster, lighter, and more energy-efficient. Additionally, graphene's flexibility and strength are being utilized in the development of flexible electronics, such as wearable devices and foldable displays, which could dramatically change how electronic devices are integrated into our daily lives.[4–7]

Graphene oxides (GO) and reduced graphene oxides (rGO) offer significant advantages in stimuli-responsive (smart) materials due to their relative cost, stability, mechanical properties (strength and flexibility), and excellent electrical and thermal conductivity, deeming them promising candidates for sensing, actuating, and hydrogel materials. These properties exhibited in graphene and chemically modified graphene (e.g., GO and rGO) overcome the limitations of conventional smart materials (such as alloys, inorganic materials, ceramics, and polymers), which face challenges such as high operation voltages, poor mechanical strength/integrity, or environmental instability.[8] Moreover, graphene and GO possess antibacterial activity against many

M. A. Saeed, Y. Alshammari, A. Alkandary
Energy and Building Research Centre
Kuwait Institute for Scientific Research
Kuwait City 12043, Kuwait
E-mail: msaeed@kisr.edu.kw

A. Abdelkader
Bournemouth University
England BH12 5BB, UK

A. Abdelkader
University of Cambridge
Cambridge CB2 1TN, UK

C. Valles
Department of Materials
National Graphene Institute and Henry Royce Institute
University of Manchester
Manchester M13 9PL, UK

The ORCID identification number(s) for the author(s) of this article can be found under https://doi.org/10.1002/mame.202400316

DOI: 10.1002/mame.202400316

types of bacteria.[9] One important mechanical distinction between graphene and GO/rGO is that the former fails inherently in a brittle fashion. Its oxidized derivatives, although less robust mechanically, contain epoxide groups that dissipate energy plastically and, hence, are relatively ductile.[10] Therefore, adding to the applicability of GO/rGO strain sensing, shape-shifting materials, soft actuators, hydrogel, and aerogel composites.

The energy sector stands to benefit significantly from graphene applications as well. Its superior electrical conductivity and large surface area make it an excellent material for the electrodes of batteries and supercapacitors, potentially leading to energy storage devices with much higher capacities and faster charging times. This could be crucial for advancing electric vehicles and renewable energy technologies.[11–14] Moreover, graphene's ability to act as a barrier while allowing certain molecules to pass through is being explored in the development of more efficient and durable membranes for water purification and gas separation, addressing some of the world's most pressing environmental challenges.[15–18]

Finally, graphene is incorporated into composite materials to enhance their mechanical, thermal, and electrical properties. These graphene-enhanced materials are finding applications in the aerospace, automotive, and construction industries, where they contribute to creating lighter, stronger, and more durable materials.

2. Graphene as Mechanical Reinforcement in Polymer Nanocomposites: The Importance of The Graphene/Polymer Interface

With a Young's modulus of 1 TPa and a tensile strength of 130 GPa, graphene is one of the stiffest and strongest known materials, making it an ideal candidate to reinforce polymers and fabricate high-performance polymer nanocomposites for applications in the automotive and aerospace industries, for example. A lot of work has already been done in recent years where polymers of different natures have been successfully reinforced by adding graphene. However, the maximum potential of this nanomaterial has not been reached yet. Indeed, even though graphene has extremely high intrinsic modulus and strength when it is incorporated into a polymer matrix as "bulk", the effective modulus is considerably lower than that theoretically predicted, suggesting that the outstanding properties of graphene are not effectively transferred from the nanoscale to the macroscale, hence, we are limited to reaching only modest levels of reinforcement. Finding answers to questions such as "How does the matrix interact with graphene particles?" and "What kind of theoretical description is appropriate?" emerge as prerequisites to a fundamental understanding of the hierarchal translation of composite properties. Thus, formulating a comprehensive understanding of and overcoming the existing limitations that hinder fully exploiting graphene as a polymer nanocomposite reinforcement.

A lot of investigation has been done in the last two decades to understand the nature of the interaction between polymers and graphene from a theoretical point of view, ergo, models have been established. Gong et al. demonstrated unambiguously that stress transfer occurs from the polymer matrix to monolayer graphene, probing that graphene can successfully reinforce polymers.[19] They also showed that continuum mechanics could be used to study graphene monolayer nanocomposites and modeled the observed behavior using shear-lag theory. In addition, they successfully monitored the stress transfer efficiency and breakdown of the graphene/polymer interface using Raman spectroscopy, which revealed that the stress transfer between graphene and polymer depends on both s (i.e., the aspect ratio of the graphene) and the parameter n (widely accepted as an adequate measure of the interfacial stress transfer efficiency, i.e., the degree of interaction between graphene and the polymer matrix).[19] They found that the interface between unfunctionalized graphene and polymer is very weak, and $ns > 20$ is required to reinforce the polymer sufficiently. Graphene flakes with relatively large lateral dimensions (aspect ratio) will contribute to the reinforcement by increasing the value of s. Alternatively, chemical modification of the surface or edges of the graphene flakes may significantly strengthen the interface between graphene and polymer, reducing the critical length (thus s) and increasing n.

2.1. Role of the Lateral Dimensions of Unfunctionalized Graphene

The role of carbon nanoparticles' length/aspect ratio on the physical properties and mechanical reinforcement of bulk polymer composites has been investigated. For example, a combination of graphite nanoplatelets and nanotubes was used to study how their particles' length affect the reinforcement of bulk epoxy composites.[20] Some works on the role of the aspect ratio/length of a few layers of graphene have also been reported. May et al. studied the effect of very low loadings (<1 wt.%) of exfoliated few-layer graphene on the properties of polyvinyl alcohol[21] composites.[22] They found reasonable levels of reinforcement of the polyvinyl alcohol[21] matrix when graphene with lateral dimensions/lengths ≥2.3 μm was incorporated into the matrix, whereas the addition of smaller flakes led to poor levels of reinforcement. The effect of the size/aspect ratio of a few layers of graphene on the reinforcement and physical properties of poly(methyl methacrylate) (PMMA) and polypropylene (PP) has also been recently studied, covering a more comprehensive range of loadings.[23,24] In these works, electrochemically exfoliated few layers of graphene with two different lateral dimensions (20 and 5 μm) and similar thicknesses were incorporated into the matrix by melt mixing using a twin-screw compounder at loadings from 0.5 wt.% to 20 wt.%. It is worth mentioning that high loadings (up to 20 wt.%) of graphene nanoplatelets were successfully incorporated into these two polymers without compromising their viscosities (as revealed by their rheological analysis), which is excellent news from an industrial point of view. The thermal stability of the PMMA determined using thermogravimetric analysis (TGA) was considerably improved by adding these two types of graphene. However, considerably higher thermal degradation temperatures (T_d) were observed for the system based on the 5 μm graphene relative to the one based on the 20 μm graphene at loadings up to 10 wt.%, as shown in **Figure 1a**. Improved thermal stabilities in polymer nanocomposites are typically attributed to the formation of a graphene network in the matrix acting as a gas barrier inhibiting the emission of gas molecules coming from the thermal decomposition of

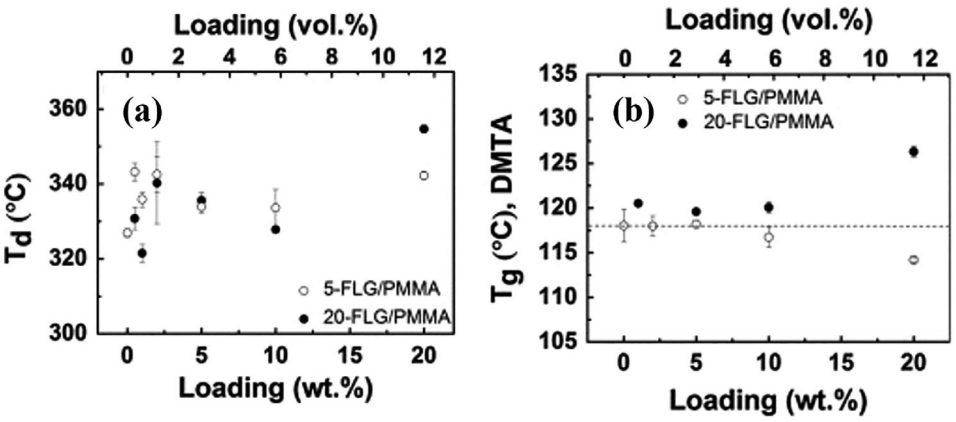

Figure 1. Variation of T_d (a) and T_g (b) of the graphene/PMMA composites with graphene loading. Reproduced with permission.[23] Copyright 2015, Elsevier Ltd.

the polymer. Hence, this enhanced thermal stability found for the smaller flakes must be related to the formation of a more effective network, probably due to the achievement of better dispersions (more π-π interactions, bending, folding, etc., are expected in the case of larger flakes due to their higher specific surface area)x. At 20 wt.%, the presence of small agglomerates in both systems, however, seems to make the higher surface area of the particles more critical than the dispersion, and the large flakes show better thermal stability than the small ones.

The glass transition temperature (T_g) determined by dynamic mechanical, thermal analysis (Figure 1b) was found to increase only when the polymer was filled with the 20 μm flakes, which suggested a better adhesion or enhanced attractive interactions between them and the polymer relative to the 5 μm flakes. This must be related to the greater surface area of the larger flakes, which facilitates the interaction/adhesion with the polymer, thus leading to stronger interfaces.

As shown in **Figure 2**, tensile testing resembled glassy polymeric behavior for both composite systems, with higher levels of reinforcement achieved for the 20 μm graphene-based one. Indeed, when the 5 μm graphene is incorporated into the polymer, Young's modulus of the polymer increases only slightly (≈7%) up to the optimal 2 wt.% loading. In contrast, the modulus of the polymer was found to increment progressively with loading up to 20 wt.% (showing an improvement of ≈74%) when the larger flakes were used. Very small increments in the tensile strength of the polymer were found for both graphene types up to 2 wt.% loading (≈5% and 3% for the 20 and the 5 μm graphene, respectively), and a progressive increase of brittleness with loading was also observed for both systems. This behavior is typically observed in polymers filled with carbon nanomaterials, and it is related to the formation of agglomerates of graphene in the matrix, deteriorating the interface between graphene and polymer.

These results demonstrate that, due to more extensive contact area, graphene materials with relatively large lateral dimensions (>20 μm) provide better interaction and interfacial stress transfer with the polymer relative to smaller flakes, leading to improved thermal and mechanical properties of the overall composites, as predicted by the shear lag theory. The question that remains open is whether incorporating functional groups on the surface and edges of the graphene flakes can further improve the mechanical properties of their nanocomposites through improved graphene-polymer interfaces.

2.2. Role of Surface Chemistry of Graphene

2.2.1. Graphene Oxide

GO represents a very simple functionalized graphene. It is typically prepared following the chemical oxidation of graphite using harsh oxidants, which leads to highly oxidized graphite oxide. Graphite oxide is still a layered structure, and it encompasses many oxygen-containing functionalities between the layers, favoring its exfoliation in water using sonication or mechanical stirring, leading to GO monolayers. They are highly oxidized graphene monolayers, encompassing many oxygen-containing functionalities on their surface and edges, both covalently attached and physically absorbed.[25–27] Due to its very rich surface chemistry, GO materials have been widely used in nanocomposites because they are expected to render better dispersions in the polymer and provide stronger interfaces, thus leading to improved levels of reinforcement relative to unfunctionalized graphene.

In addition, GO can be chemically or thermally reduced to partially remove those functional groups from the surface of the flakes, reducing the amount of oxygen-containing functionalities and, thus, restoring the Csp^2 network typical of graphene.[28] The graphene material resulting from these reductions (i.e., rGO) is electrically conductive. In contrast, GO is not due to the presence of all those functionalities on the surface of the flakes. Alternatively, GO can be "washed" using a base (e.g., NaOH) to remove the functionalities that are physically adsorbed on the surface of the flakes, rendering a GO-derived material ("base washed GO", bwGO) that contains considerably lower amounts of oxygen and is also electrically conductive.[25] (The structure of bwGO is schematically shown in **Figure 3**).

All these GO-derived materials (i.e., as-prepared GO, rGO, and bwGO) have been widely used to reinforce polymers of different natures and the influence of their different surface chemistries

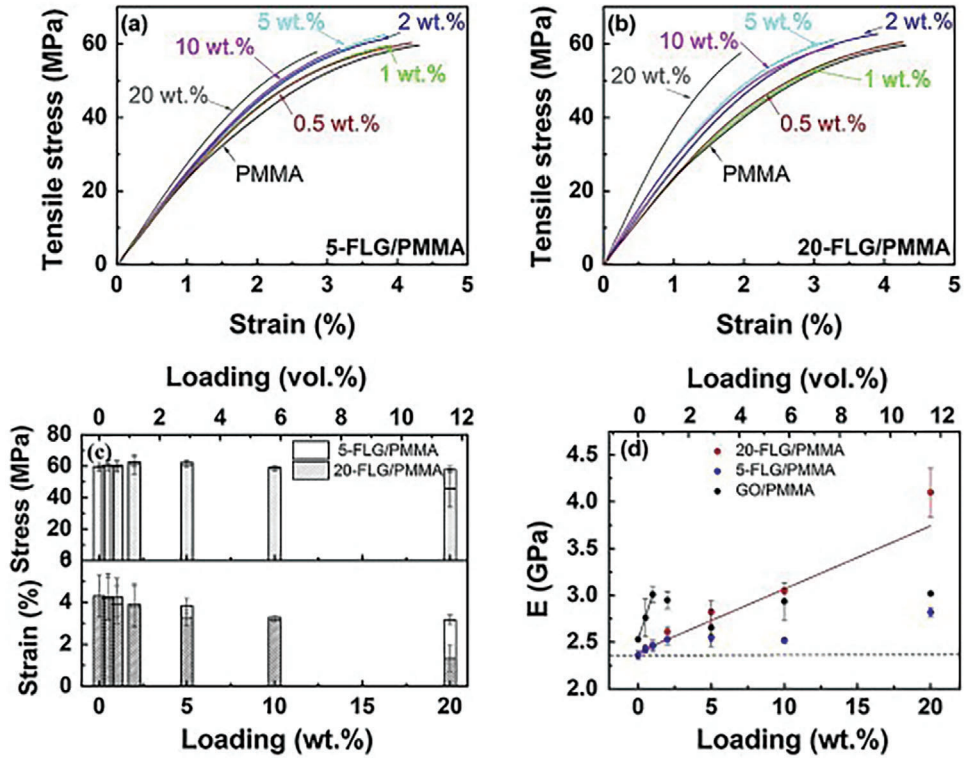

Figure 2. Stress–strain curves of 5 µm-graphene (5-FLG)/PMMA a) and 20 µm-graphene (20-FLG)/PMMA b) nanocomposites at different loadings; c) Variation of the stress and strain at break of the composites with loading; d) Variation of Young's modulus with loading for the 20 µm graphene and the 5 µm graphene (they are compared with the GO-based system). The dotted line corresponds to the modulus of the neat PMMA. Reproduced with permission.[23] Copyright 2015, Elsevier Ltd.

on the dispersion, graphene-polymer interface and, thus, on the thermal and mechanical properties of their nanocomposites have been investigated. It has been recently reported that the interface between GO and a PMMA matrix is stronger than that between bwGO and PMMA due to the presence of a higher number of functionalities on the surface of the flakes before the base washing.[29] This improved interface was found to favor the dispersion of the flakes in the matrix, leading to enhanced thermal stabilities (through the formation of a well-distributed network of graphene in the matrix acting as a gas barrier inhibiting the emission of gas molecules coming from the thermal decomposition of the polymer, as mentioned above), and improved T_g (clearly suggesting stronger interfaces and better adhesion between filler and polymer, thus impeding the movement of the polymer chains up to higher temperatures), as shown in **Figure 4**.

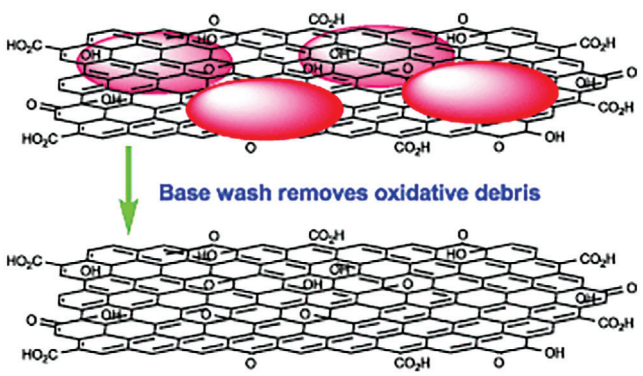

Figure 3. The schematic shows the structure of as-prepared GO and bwGO. Reproduced with permission.[25] Copyright 2011, John Wiley and Sons.

As seen in **Figure 5**, the addition of both fillers successfully reinforced the polymer up to the optimal 1 wt.% loading, making the composites' overall performance slightly better when GO was used relative to bwGO at the same loading. The PMMA modulus was found to increase by ≈38%, and ≈28% for as-prepared GO and bwGO, respectively, and the strength at break of the polymer was only increased for the GO-based system (21% improvement was observed for 1 wt.% loading of GO). These results suggest that the stronger interface between the polymer and highly functionalized GO favors the mechanical reinforcement of the polymer. It is worth mentioning, though, that the difference in the mechanical properties observed between these two systems is relatively small because bwGO flakes still contain functionalities on their surface (it is not completely "washed"; only the physisorbed groups are removed, whereas some covalently attached groups remain, favoring the interaction with the polymer). However, for loadings above the optimal 1 wt.%, the graphene-graphene interactions started to dominate the system over graphene-polymer interactions, hence promoting the agglomeration of graphene through π-π and van der Waals interactions, impeding any further improvement of the mechanical

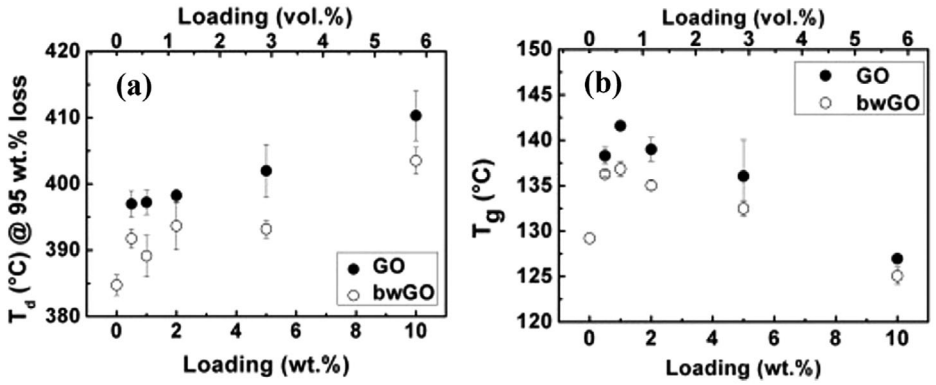

Figure 4. Variation of T_d (a) and T_g (b) of the GO/PMMA and bwGO/PMMA composites with filler loading. Reproduced with permission.[29] Copyright 2013, Elsevier Ltd.

performance of the overall composite at higher loadings, as shown in Figure 5d.

Figure 6 compares the relative modulus (E/E_0) found for this GO-based system with those based on unfunctionalized graphene (described in Section 2.1). It can be seen that the addition of unfunctionalized flakes with small lateral dimensions (5 μm) led to poor levels of reinforcement. Larger flakes are needed (≥ 20 μm in diameter) to be above the critical length and to achieve significant levels of reinforcement, with the modulus of the polymer increasing linearly up to relatively high loadings (20 wt.%). From Figure 6, it is evident that the incorporation of GO leads to stronger interfaces with the polymer due to the presence of a high number of functionalities on the surface of the flakes, which leads to higher levels of reinforcement relative to unfunctionalized graphene. However, this only seems to happen at relatively low loadings, up to the optimal 1 wt.%, due to the tendency of GO flakes to agglomerate above that critical loading. The presence of those oxygen-containing functionalities on the surface and edges of GO flakes seems to promote stronger interfaces with the polymer (relative to unfunctionalized graphene) at low loadings, but at the same time, that rich chemical surface is promoting flake-flake interactions at loadings above the optimal loading, leading to the formation of small agglomerates of GO in the polymer matrix through Van de Waals forces and π–π

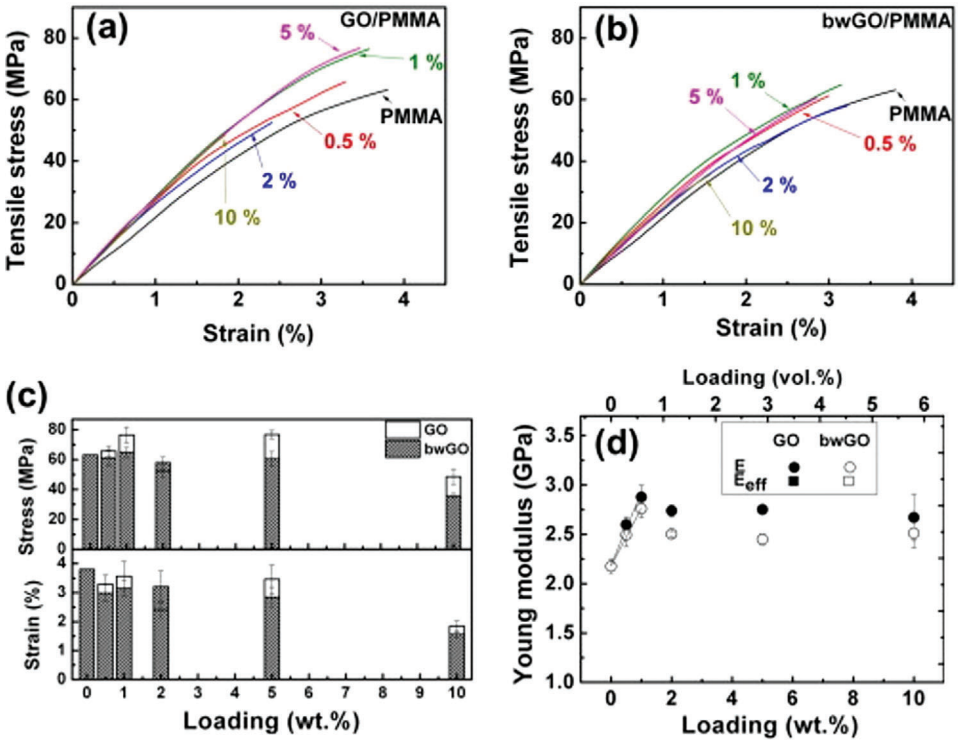

Figure 5. Stress–strain curves of a) GO/PMMA and b) bwGO/PMMA nanocomposites; c) Variation of the stress and strain at break of the nanocomposites with filler loading; d) Variation of Young's modulus of the nanocomposites with filler loading. Reproduced with permission.[29] Copyright 2013, Elsevier Ltd.

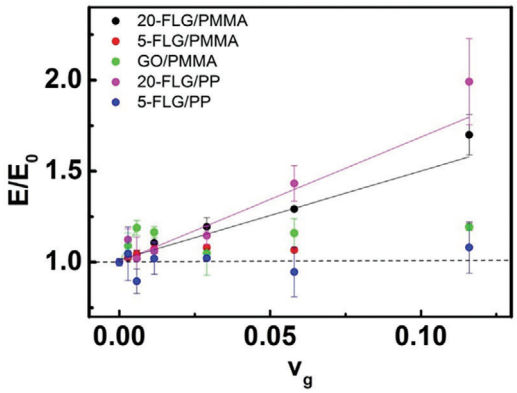

Figure 6. Variation of E/E_0 with loading for different graphene/polymer systems. Reproduced with permission.[24] Copyright 2014, Faraday Division, Royal Society of Chemistry.

interactions, and impeding further improvements on the mechanical properties of the overall composites. Ideally, we would like to design graphene flakes that can interact strongly with polymers while minimizing flake–flake interactions as the filler loadings are increased so that the reinforcement can be improved further. The key question that emerges now is: what is the right level of functionalization for that?

2.2.2. Polymer Grafting

Controlled functionalization of graphene materials where functional groups (other than the oxygen-containing groups present on the surface and edges of GO) could prevent the undesired agglomeration typically observed for GO at loadings above 1 wt.% through steric stabilization whilst still providing a strong interface between filler and polymer, emerges as a good solution to further enhance the mechanical and thermal properties of graphene/polymer nanocomposites. For example, the grafting of aryl groups on GO-derived materials has successfully improved the thermal and mechanical properties of polymer composites through enhanced compatibilities and stronger filler-polymer interfaces.[30–32] However sometimes, mainly when non-polar polymers are used as the matrix, those strategies are not enough to achieve good levels of dispersion and strong enough filler-polymer interfaces, and polymer functionalization is required.[33]

The synthesis of polymer-grafted GO materials and their incorporation into host polymers of different nature (e.g., polyetheramine-functionalized GO into an epoxy resin,[34] epoxy-grafted GO into a PC matrix[35] or nylon 6-grafted-GO into a nylon matrix[36]) has been reported to improve the mechanical and thermal properties of their composites through enhanced compatibilities and stronger filler/polymer interfaces relative to the non-modified graphene materials. Some approaches to enhance the compatibility and interface between graphene and thermoplastic polymers have also been recently reported, including PMMA-functionalized exfoliated graphene,[37] PMMA-grafted chemically reduced GO,[38] or PMMA-grafted GO,[39,40] also leading to improved thermal and mechanical properties. Further to GO-derived materials, a chemical strategy to fabricate covalently bonded PMMA-grafted commercially available graphene nanoplatelets has recently been reported to enhance the performance of PMMA nanocomposites.[41] In this work, graphene nanoparticles (GNPs) grafted with PMMA chains were prepared using a simple diazonium coupling reaction to give NH_2-terminated flakes followed by an amidation reaction between the NH_2 groups and the PMMA chains (PMMA-NH-GNPs), as schematically shown in **Figure 7**.

When as-received GNPs and PMMA-grafted GNPs were incorporated into a PMMA matrix, enhanced thermal stabilities, and increased T_g were found for the system based on the chemically modified graphene relative to both pure polymer and the as-received GNPs-based system, as shown in **Figure 8**. The values found for T_d of this system based on modified GNPs (i.e., the T_d of the polymer was increased by 29 °C with the addition of 5 wt.% loading of the PMMA grafted GNPs) were much higher than those typically found for unmodified GNPs and GO derived materials. (Please note that these commercially available GNPs are different from the electrochemically exfoliated graphene nanoplatelets discussed in Section 2.1. Thus, the improvements in T_g, for example, are not precisely the same in both cases).

As seen in **Figure 9**, the addition of PMMA-grafted graphene into a PMMA matrix led to essential improvements in the mechanical properties of the polymer (including Young's modulus, stress, and strain at break) up to the optimal 2 wt.% loading. In contrast, poor levels of reinforcement could be seen when the unmodified GNPs were incorporated into the polymer at all studied loadings. It is worth highlighting that these polymer-grafted graphene fillers rendered improvements in the strength and strain at break (in addition to improvements on the polymer modulus), which was not observed for unmodified graphene or GO-derived materials. In addition, by using this polymer-grafted graphene, the optimal loading increased to 2 wt.% (from the optimal 1 wt.% typically found for GO). Further increases in the optimal loading and physical properties of these composites are to be expected once these chemical processes are optimized.

The improved thermal and mechanical performances observed for the polymer-grafted materials relative to other types of graphene are attributed to enhanced compatibility with the polymer, which leads to improved dispersions of the flakes in the matrix and stronger graphene/polymer interfaces. A strategic choice of the nature and amount of the grafted polymer chains for a particular host polymer will allow us to tune the graphene/polymer interface and thus control the nanocomposites' physical properties, which will open the door to a wide range of new applications in the field of graphene-based nanocomposites.

2.2.3. Polymer Self-Assembly

As covered in the previous sections of this review, most of the work reported on the mechanical reinforcement of polymers by adding different types of graphene as nanofiller focuses on the incorporation of relatively small amounts of chemically modified particles, which lead to important improvements in the mechanical properties of the polymer through strong interactions with the polymer matrix and a good load transfer. However, the optimal filler loading on those nanocomposites is typically limited to ≈1—2 wt.%, with the improvement of the nanocomposite's

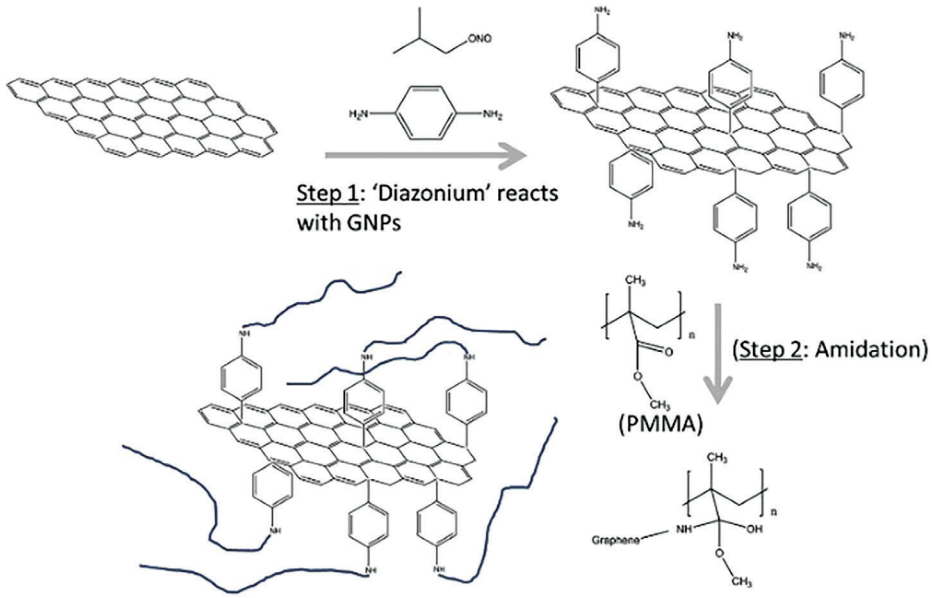

Figure 7. The scheme of the reaction was developed to fabricate PMMA-grafted GNPs. Reproduced with permission.[42] Copyright 2019, Elsevier Ltd.

mechanical properties above such optimal loading being challenging. This limitation in filler loading, hence on the levels of mechanical reinforcement that can be achieved, is mainly due to the interactions between individual chemically modified graphene flakes, which lead to the formation of agglomerates in the polymer matrix when such interactions are weaker than the interactions between filler particles and polymer, as well as to the isotropic nature of these graphene reinforced nanocomposites (i.e., the random orientation of the flakes in the matrix).

To overcome those limitations and achieve higher filler loadings, superior levels of mechanical reinforcement and new processing strategies that produce highly aligned and closely packed nanofiller particles have been recently reported. The most common method for processing polymer nanocomposites with high loadings (≈50 wt.%) of highly aligned nanofiller particles is layer-by-layer assembly (LBL), which is based on a methodical layering of polymers and nanoparticles by exposing a particular substrate to alternating solutions of these two components. The formation of a layered structure is induced during the assembly process by strong attractions between those components, which are also responsible for reinforcing the final nanocomposite structure. This technique has been probed to lead to strong clay-based polymer nanocomposite materials with very high moduli, as a consequence of both the high alignment of the nanofiller particles (highly ordered layered structures) and the possibility of achieving very high overall nanofiller loadings.[43–45]

Vacuum-assisted self-assembly (VASA) has also been recently reported as a highly flexible technique for fabricating well-ordered, freestanding GO/polymer nanocomposite films and papers with high nanofiller concentrations (>50 wt.%).[46,47] Such materials, with significant contents of both polymer and nanofiller, can be easily obtained by filtering a colloidal solution of GO that has been pre-dispersed in a polymer-containing host solution through a membrane filter. VASA has been reported to successfully produce macroscopic samples of homogeneous layered GO/polymer nanocomposites with either hydrophilic or

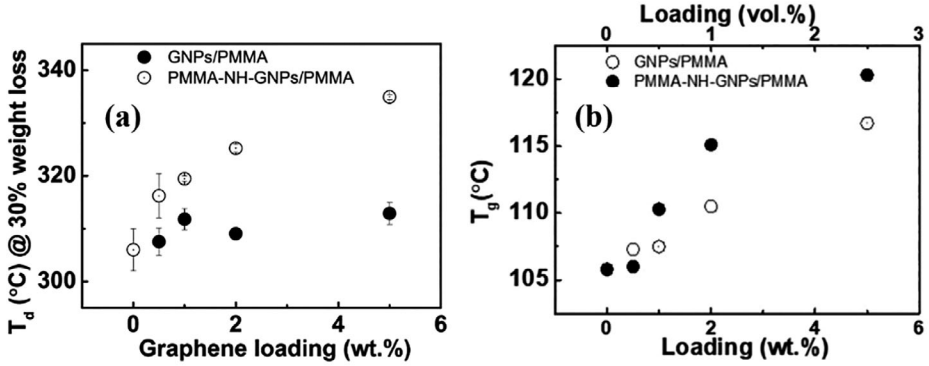

Figure 8. Variation of the T_d (a) and T_g (b) with loading for the GNPs/PMMA and PMMA-grafted GNP/PMMA composite systems. Reproduced with permission.[42] Copyright 2019, Elsevier Ltd.

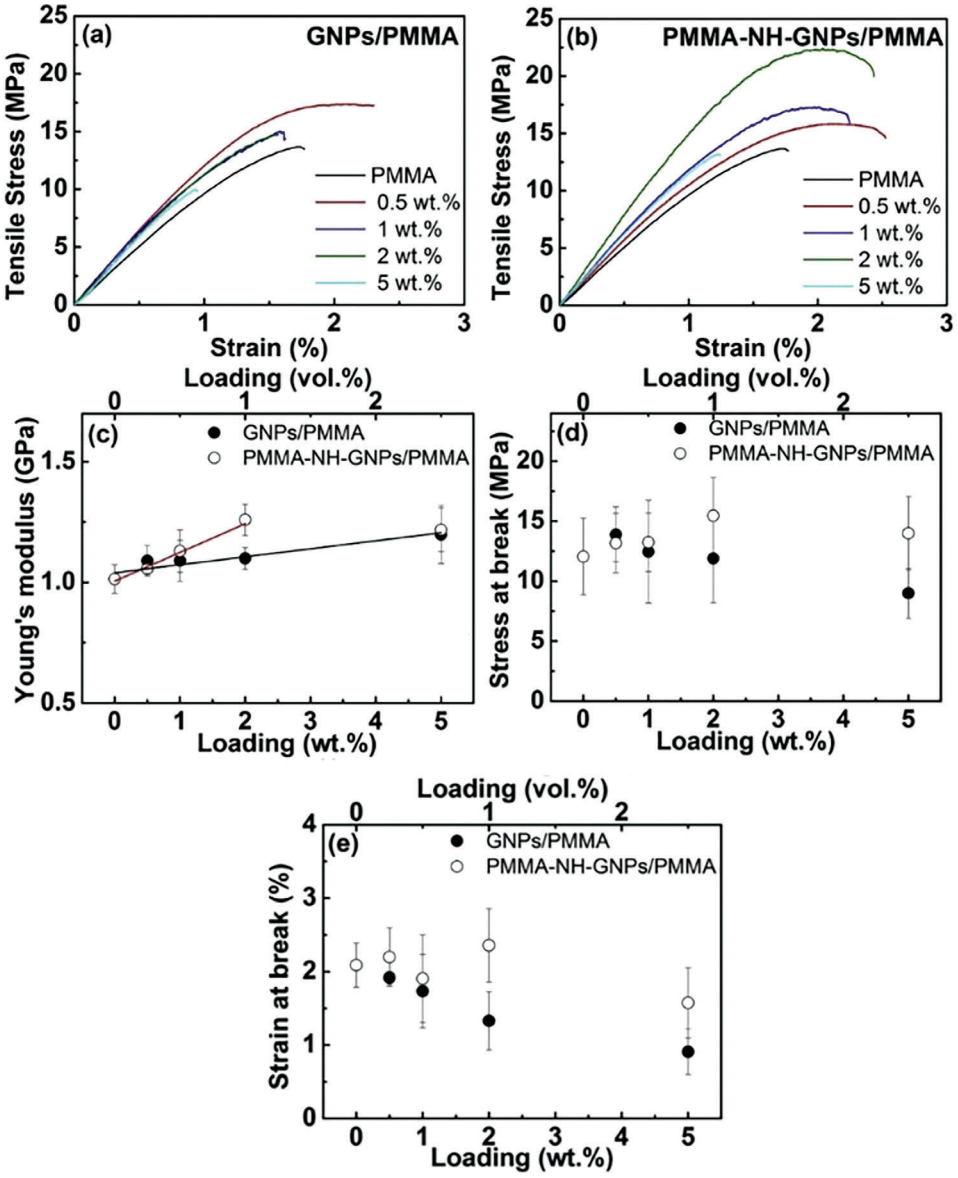

Figure 9. Stress–strain curves were obtained for GNPs/PMMA a) and PMMA—NH—GNPs/PMMA b) composite systems. Variation of Young's modulus c), stress at break d), and strain at break e) with loading for the two systems studied. Reproduced with permission.[42] Copyright 2019, Elsevier Ltd.

hydrophobic polymers very quickly, rendering excellent mechanical properties. This technique relies on filtration for assembly of the nanocomposite structure instead of alternating layer deposition, hence it can be envisioned as a complimentary method to LBL for the fabrication of layered polymer nanocomposites, expanding the scope of those LBL layered materials and allowing a wider range of possibilities to design a nanocomposite with the mechanical properties required for a particular application.

3. Graphene and Graphene Derivatives in Energy Storage

Large-scale energy storage systems are important in tomorrow's electrical power grid. They provide grid stability, security, and reliability, particularly in supporting intermittent renewable resources.[48] At the forefront of energy storage systems are electrochemical energy storage methods, which offer high energy density, flexibility, scalability, and pollution-free operation.[49] Batteries are compact, flexible, and lightweight, making them excellent power sources for handheld devices, electric vehicles, and stationary grid applications. Sodium/sulfur (Na/S) battery technology is now available for use in the grid, with ≈200 installations around the world that provide a total discharge power capacity of 315 MW. Next, lead-acid batteries have a total discharge capacity of 35 MW.[50] Nevertheless, existing battery technologies are unable to fulfill the demands for durability, high-power performance, round-trip energy efficiency, and/or cost-effectiveness needed for extensive energy storage.[51] Lead-acid batteries experience a brief cycle life, even when discharged only to a

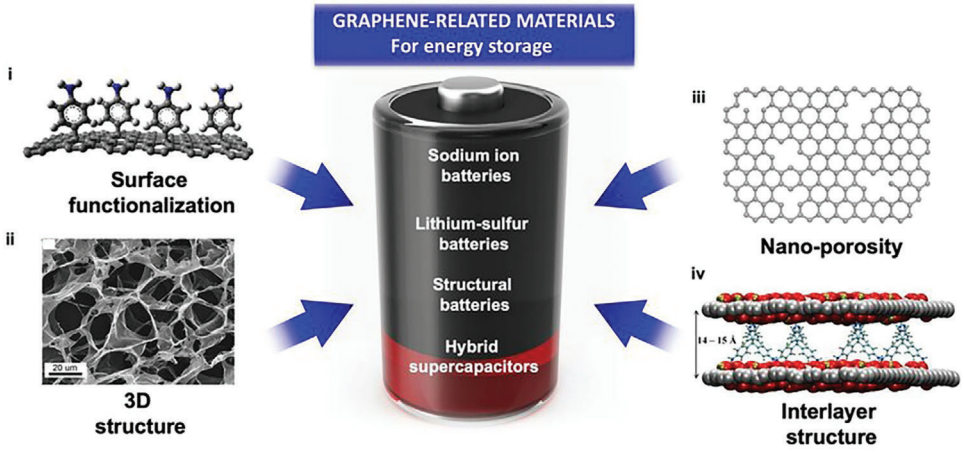

Figure 10. Some typical structures and applications of graphene-related materials. Reproduced with permission.[56] Copyright 2023, Royal Society of Chemistry.

limited extent.[52] Redox flow batteries, like the Na/NiCl2 "Zebra" battery, along with several variations of the traditional lead-acid system, are unable to function at sufficiently high rates. Na/S batteries are far too costly, as are the metal hydride/nickel batteries utilized in hybrid vehicles at this time. Lithium-ion batteries, which currently lead the market for portable electronics and electric cars, have started to make inroads into the grid-scale stationary energy storage sector.[49] Lithium-ion batteries possess a high voltage and energy density, exhibit low self-discharge rates, and demonstrate outstanding rate performance.[53] However, the initial experimental data in the field showed that Li-ion batteries require enhancement in capacity and durability. In addition, conventional lithium-ion batteries suffer from high cost and some safety problems.[54]

In many battery systems, graphene can play significant roles in enhancing the battery's performance, either as an active electrode material or as an additive. The unique set of properties of graphene, particularly its high conductivity, chemical, and electrochemical inertness, large specific surface area, and ultimate thin planer structure, made it an ideal candidate for many energy storage applications (**Figure 10**).[55] Graphene and graphene additives have been used in the electrodes of metal-ion batteries, metal-air batteries, supercapacitors and metal-ion hybrid capacitors, alkali metals-sulfur batteries, and solid-state batteries. Graphene has also been used as a modifier for the separator of metals-sulfur and solid-electrolyte batteries.

The next sections are devoted to investigating the applications of graphene in various battery systems.

3.1. Graphene for Lithium-Ion Batteries

Graphene has been widely studied as a potential material for Li-ion batteries due to its high surface area, excellent electrical conductivity, and mechanical strength. It is a promising anode chemistry for lithium-ion batteries due to its high lithium-ion storage capacity and excellent life. Graphene's high electrical conductivity allows for faster charge/discharge rates and improved power output. Additionally, the large surface area of graphene allows for more efficient utilization of the active materials in the battery, which can lead to higher capacity and energy density. Another potential benefit of using graphene in lithium-ion batteries is its excellent mechanical strength, which allows it to withstand the stresses of charge/discharge cycling and can help extend the overall lifespan of the battery.

Despite these promising properties, there are still some challenges to overcome in the development of graphene-based lithium-ion batteries. One of the main challenges in using graphene as an anode material is its relatively low lithium-ion diffusivity, which can lead to slow lithium-ion transport and low-rate performance. Researchers have attempted to overcome this challenge by using various techniques such as synthesizing graphene with a high aspect ratio, synthesizing hybrid materials of graphene and other materials, and using graphene-based composite materials.[57,58] In a recent study, holey graphene (HGs) was prepared and used in a low quantity (1 wt.%) as conductive additives in $LiFePO_4$ battery in addition to 1 wt.% of carbon black as super-P (SP) which led to high energy density and excellent rate performance similar to the one when 10 wt.% of SP is added (**Figure 11**).[59]

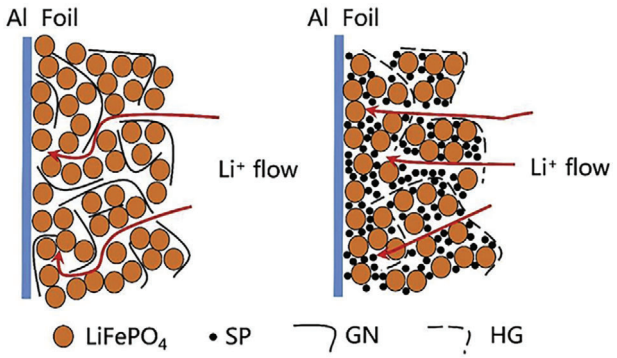

Figure 11. Schematic diagrams of the lithium-ion transportation paths in $LiFePO_4$ cathodes with graphene nanosheets (GN) or HG in addition to SP as the conductive additives. Reproduced with permission.[59] Copyright 2019, Elsevier Ltd.

Another challenge in using graphene in lithium-ion batteries is the limited availability of high-quality graphene, which can be difficult to produce in large quantities. Additionally, the cost of graphene is currently quite high, which may limit its widespread use in commercial applications. Moreover, its high-volume expansion upon lithiation can lead to mechanical degradation and capacity fading over time. There have been several approaches to overcome these challenges, including expanding the interlayer space in few-layer graphene, the use of graphene hybrids with other materials, graphene composites, and graphene-based coatings. Graphene hybrids have been prepared by combining graphene with other materials, such as metal oxides, polymers, and carbon nanotubes, which can improve the stability and conductivity of the graphene. Graphene composites have also been prepared by incorporating graphene into a matrix material such as a polymer or ceramic, which can improve the mechanical properties and capacity retention of the graphene. Graphene-based coatings have been applied to the surface of electrodes to improve the charge/discharge rate and capacity retention of the battery.

One of the most promising hybrids of graphene is the silicone graphene system. Silicon and graphene can be blended to form a single nanocomposite, and this was found to be one of the early approaches to producing Gr/Si composite anode. It is still attractive as a simple and efficient staggering. Graphene matrix provides the following benefits: physical support to Si nanomaterials, a cushion to buffer massive Si volume change, and a conductive pathway to carry the charges. Lee and co-authors were able to develop one of the successful early Si/Gr composite anodes for the LIBs.[60] In this study, the Si/Gr composite was fabricated by a simple dispersion of Si particles in graphene sheets. The graphene was synthesized by H_2 reduction of Si/GO composite from raw graphite, and commercial Si nanoparticles (size less than 30 nm) and PVDF binder were used as raw materials. The nanocomposite exhibited a superior initial capacity of 4200 mAh g^{-1} at 1 A g^{-1} after 50 cycles and a stable reversible capacity of 1500 mAh g^{-1} after 200 cycles. The encouraging cycle life proved that the sandwiching of Si nanoparticles within the graphene network is a viable strategy to control Si volume change to some extent due to excellent mechanical support and high conductivity. The authors further claimed that the homogenous distribution of Si NPs in graphene sheets, thinner graphene flakes, high crystallinity, and conductivity play a vital role in achieving high electrochemical performances. In another experiment, the authors experimented with the effect of surface functionalization of Si/graphene on electrochemical performances. In this study, the NPs surface has converted into hydrophobic Si-H groups by the HF etching technique while graphene has converted into phenyl isocyanate capped rGO, as explained by Stankovich et al. Despite the surface modification, the resulting anode could only deliver a capacity of ≈200 mAh g^{-1} after 20 cycles at 100 mA g^{-1} of current density, which is approximately one-third of the non-functionalized Gr/Si nanocomposite. In summary, the commercial feasibility of this work was found to be quite tricky due to the involvement of complex synthesis procedures and flammable H_2. Moreover, the role of rGO particle properties was studied in Si/rGO composite electrodes providing a uniform solid electrolyte layer in Li-ion battery. It was found that decreased structural defects in rGO led to 84% initial columbic efficiency while more spheric rGO particles led to a more stable cycle life showing 93% capacity retention after 100 cycles (**Figure 12**).[61]

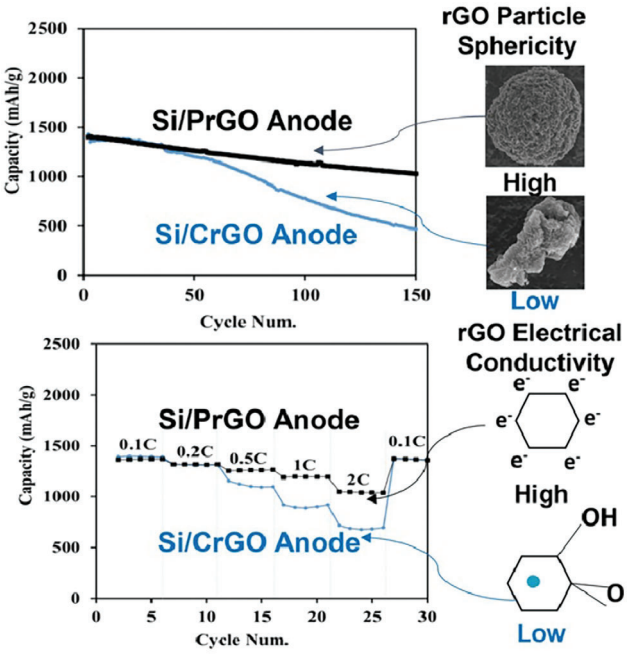

Figure 12. Comparison between capacity retention in Si/rGO electrodes showing the effect of rGO particle sphericity and electrical conductivity. Reproduced with permission.[61] Copyright 2022, Elsevier Ltd.

As an alternative, Wang et al. introduced a simple filtration technique followed by hydrazine reduction to produce a flexible, free-standing Si/Gr nanofilm.[62] The composite was fabricated through hydrazine reduction of GO/ commercial Si NPs, where GO was prepared from modified Hummers oxidation of natural graphite. The following graphene/Si paper has shown a charge storage of 708 mAh g^{-1} for 100 cycles. Nevertheless, in terms of capacity and cycle life, it did not see any improvement compared to the early findings of Lee et al., and the massive, irreversible capacity loss during the first cycle has been considered a crucial limitation.[60] However, these two findings intensively highlighted the advantages of co-utilization of Si with graphene for a stable capacity.

Sun et al. proposed an in situ plasma-assisted mechanical milling approach (**Figure 13**) to increase the dispersity of Si NPs in the graphene sheets.[63] The resulting Si NP/graphene nanocomposite (20 h milled) was able to deliver a specific capacity of 976 mAh g^{-1} at 0.5 A g^{-1} after 50 cycles. However, the electrode at a full-cell design with a commercial $LiMn_2O_4$ cathode could only deliver a capacity of 150 mAh g^{-1}, which is more than six times lower than the half-cell value. A later study by the same research group in 2016[64] found that cyclability could be increased by using commercial expanded graphite (EG) instead of flake graphite and subsequent plasma-assisted milling (p-milling) with Si NPs. In this approach, expanded graphite would generate an efficient exfoliation due to its loosened and porous structure and hence guarantee the effective wrapping of Si NPs leading to a longer cycle life. The enhanced reversible capacity of the composite was 942 mAh g^{-1} at 0.2 A g^{-1} up to 100 cycles with 88% capacity retention, and a superior charge capacity

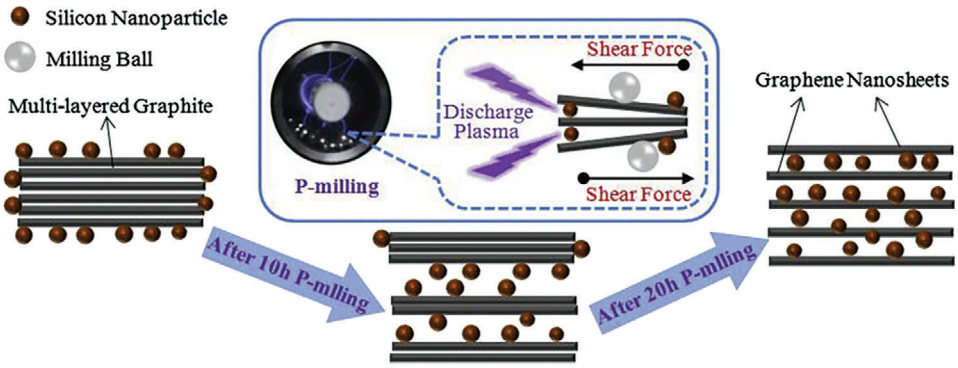

Figure 13. Schematic illustration showing the process of preparing Si/GNs composites using plasma-assisted milling. Reproduced with permission.[63] Copyright 2014, Elsevier.

of 1000 mAh g^{-1} at 0.2 A g^{-1} was found after 150 cycles. This enhanced performance again evidenced the very well-coated Si as a crucial factor in achieving longer cycle life.

Recently, Liu and co-authors introduced a hydrothermal-assisted sodium borohydride reduction of GO/Si nanocomposite as an advanced optimized approach to producing rGO/Si anode.[65] The denoted 10rGO/Si-600 (quality ratio 10, calcined at 600 °C) composite experienced an excellent initial CE of 93.2% with a reversible specific capacity of 2317 mAh g^{-1}. The cycling retention was found to be 85% with a specific capacity of 728 mAh g^{-1} over 100 cycles at a current density of 0.1 A g^{-1}.

3.2. Graphene in Metal-Air Batteries

Metal-air batteries, especially the Li-air and Na-air batteries with high theoretical specific energy (3505 and 1105 Wh kg^{-1} for Li-O_2 and Na-O_2 batteries, including the O_2, respectively), are considered the best candidates for future electric vehicles. Alkaline metal-air batteries are still in the R&D stage and suffer several problems that slow down their commercialization. These batteries usually suffer from the sluggish kinetics of ORR/OER, low conductivity of the discharge products, blocking the pores of air electrodes by discharge products, microscale size of discharge products, especially in Na-air batteries, instability of battery and electrolyte evaporation because of the open system, and dendrite growth on the anode surface. These problems cause high overpotential during discharge/charge and short cycle life. The use of a graphene-based electrocatalyst was recently proven to be a promising method to facilitate the ORR and OER, but usually, the reported electrocatalyst can alleviate the sluggish kinetics of ORR or OER alone. Cetinkaya et al. used a flexible GO paper as the cathode for Li-air batteries.[66] The porous nature of the GO paper facilitates O_2 diffusion, easing the formation and decomposition of Li_2O_2. However, in most cases, graphene or graphene derivatives worked as supporters for the metals or metal oxide nanoparticles.

Hybrids of graphene and Co_3O_4 are amongst the most studied electrocatalysts for metal-air batteries. Nezar et al. reported a reduction of 400 mV in the overpotential when Co_3O_4/RGO was used, compared to the Ketjen Black electrode. Peng et al. prepared Co_3O_4/GN composites with different Co_3O_4 loadings in an attempt to optimize the catalysts' composition.[67] They concluded the composite in 48.2:51.8 (w/w) is the optimal composition with an overpotential as low as 1539 mV (compared to 2088 mV for pristine carbon cloth). Interestingly, the overpotential increased only to 1663 mV after 300 cycles, indicating good electrode stability. In an attempt to improve the catalysis performance, Ren et al. prepared a porous graphene nanosheet hybridized with Co_3O_4 through a laser-induced process.[68] The battery with Co_3O_4/LIG electrode showed a voltage gap of the charge/discharge process at the 1st cycle was as low as 0.42 V. The battery also showed excellent cyclic performance with a capacity of over 430 mAh g^{-1}, which was maintained after 242 cycles (**Figure 14**).

Other metal oxide composites with graphene have also been investigated in the literature. The catalytic performance of manganese oxide with different phases and morphologies has been evaluated by several groups.[69–71] For example, MnO_2@rGO nanocomposite prepared by Zhu et al.[21] displayed an initial capacity of 5139 mAh g^{-1} at 100 mA g^{-1} but could only be cycled for 15 cycles.[21] Liu et al. prepared $CuCr_2O_4$@rGO composites via hydrothermal processes followed by a calcination step.[72] The composite showed excellent cyclic performance with a fixed capacity of 1000 mAh g^{-1} for over 100 cycles. Palani et al. also prepared a porous $NiCo_2O_4$ (NCO)@GNS nanocomposite via a hydrothermal process. The NCO@GNS electrode showed a discharge capacity as high as 7201 mAh g^{-1} at 100 mA g^{-1} and could be cycled over 200 cycles. Jiang et al. prepared CeO_2 microspheres anchored on graphene foams. The porous structure of the foam facilitates O_2 diffusion in addition to the flexibility of the electrode.[73] The CeO_2-graphene could deliver a discharge capacity of 3250 mAh g^{-1} at a current density of 200 mA g^{-1} and could also be cycled for 80 cycles after over 1000 folding cycles. Feng et al. synthesized a sandwich structure of multi-layered Fe_2O_3/graphene nanosheets (Fe_2O_3/GNS).[74] The delivered initial capacity was 4587 mAh g^{-1} at 100 mA and could maintain a high capacity of 959 mAh g^{-1} at 500 mA, indicating good rate capability, thanks to the mesopores structure.

3.3. Graphene-Based Supercapacitor

Graphene is considered to be a strong candidate for fabricating high-performance electrochemical double-layer (ECDL)

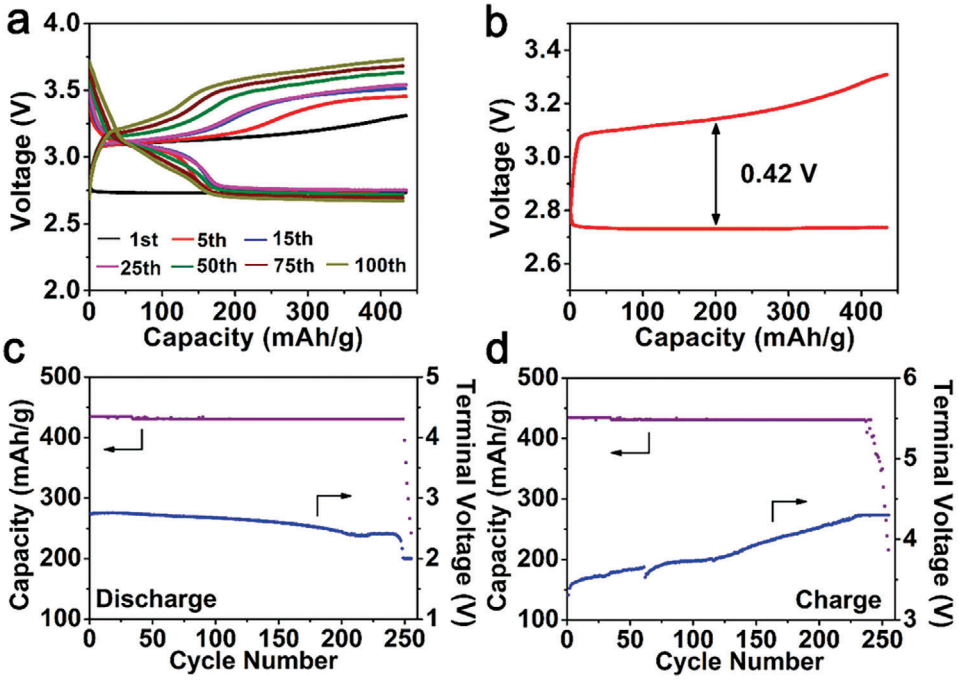

Figure 14. Characterization of the Co_3O_4/LIG Li-O_2 battery. a) Galvanostatic cycling performance of the Co_3O_4/LIG electrode at a current density of 0.08 mA cm^{-2} with a limited capacity of 430 mAh g^{-1}; b) first discharge and charge profile of the cyclic performance; c) discharge capacity and terminal voltage vs cycle number; d) charge capacity and terminal voltage vs cycle number. Reproduced with permission.[68] Copyright 2018, Elsevier Ltd.

supercapacitors because of its low mass density, excellent electrical conductivity, and high theoretical specific surface (≈2600 m^2 g^{-1}).[1,75–77] The theoretical capacity calculated for graphene-based on this specific surface area is 550 F g^{-1}. However, most of the reported specific capacities of pristine graphene are less than half of the theoretical value. The aggregation and re-stacking of the graphene flakes reduce the accessible part of the electrode, decreasing the specific capacity. Free-standing graphene foam grown by chemical vapor deposition (CVD) has shown high rate capability and is also one of the highest reported capacities for pure graphene, reaching 240 F g^{-1}.[78] However, the high cost of the graphene deposited by CVD compared with other carbon materials makes the theme impractical from the commercial point of view. rGO represents a cheap alternative that can be produced in large quantities. For example, graphene hydrogels synthesized by reducing GO with hydrazine or hydroiodic acid-produced materials gave a high specific capacitance of 220 F g^{-1}.[79,80] However, due to the presence of a high content of oxygen functional groups, the electrode conductivity was low, and the devices lost 30% of their capacitance in the first few hundred cycles. Synthesis of rGO through thermal reduction at temperatures above 1000 °C produced materials that can deliver a specific capacitance of 177 F g^{-1}.[81] Reducing GO with microwave irradiation was reported by several groups. The produced rGO exhibits good cyclability with specific capacitance between 200 and 210 F g^{-1}.[82] Using corrugated and crumbled graphene was proven to be an effective solution to prevent graphene aggregation in the electrode. Removing the oxide functional groups with reactive metals in molten salts or via direct electro-deoxidation produced crumbled graphene sheets with internal strain.[76,83] The produced materials showed outstanding cyclic stability with specific capacitance as high as 255 F g^{-1}. Also, activating the graphene sheets using KOH or acid thermal treatment increased the surface area and enhanced the specific capacitance.

Increasing the specific capacitance of the supercapacitors is also possible through hybridizing the graphene with a source of pseudocapacitance or doping the basal plane with elements such as N, P, S, and/or B. Graphene nanocomposites with metal oxides such as TiO_2, MnO_2, SnO_2, ZnO, or Co-Ni binary oxide has been reported to increase the specific capacitance.[84–87] Graphene/Co-Ni Oxide could reach a capacitance as high as 1266.7 F g^{-1} and could sustain a high current density of 1 A g^{-1}. Structures based on binary oxides could also deliver high energy densities, unlike the case with pure graphene. Nano-cubes of $NiFe_2O_4$ on rGO deliver a remarkable energy density of 50 Wh kg^{-1}.[88] However, the mechanical and electrochemical stability of graphene/metal oxide composites is always questionable, particularly for flexible devices. Doped graphene with N, B, S, and/or P may represent a more mechanically stable alternative due to the strong bond between these elements and C.[89] N-doped graphene was prepared via two main routes: i) direct synthesis starting from carbon and nitrogen raw materials such as CVD[90] or segregation growth and arc-discharge[91,92] and ii) post-preparation treatment where graphene is treated in the presence of a nitrogen source in processes such as hydrothermal treatment, thermal annealing, plasma treatment, or molten salts electrochemical doping.[89,93,94] For example, the electrochemically doped graphene electrodes could deliver a specific capacitance of 320 F g^{-1} and maintain 96% of this value after 10000 cycles (**Figure 15**).

The ultimate planar structure of graphene, along with its unique mechanical strength and ductility, makes it one of the

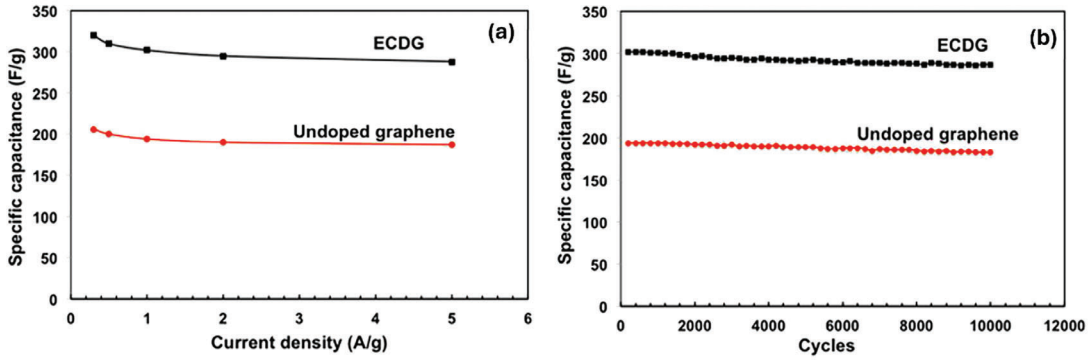

Figure 15. Electrochemical performance of electrochemical doped graphene (ECDG) electrodes; a) change of specific capacitance with current density for both ECGD and undoped graphene, and b) cyclic stability of the ECDG and the undoped graphene electrodes. Reproduced with permission.[95] Copyright 2017, Royal Society of Chemistry.

most suitable candidates for flexible devices, including supercapacitors. Various materials have been used as current collectors and substrates to fabricate flexible graphene electrodes, such as PET, nickel foam, carbon cloth, aluminum foam or foil, graphite paper, carbon nanofibers, and textiles.[96] Textiles offer additional advantages in terms of flexibility and biocompatibility, making them ideal substrates for wearable applications.[97] Another advantage of textiles is their porous structure, created by weaving or pressing natural or synthetic fibers, which allows for maximum contact between the electrode and the electrolyte.[98] Textiles, particularly those from natural sources, have numerous functional groups on their surface, including hydroxyl groups, which provide suitable links with the functional groups on the GO surface.[99] This link enhances adhesion between the graphene and the substrate, producing electrodes with long cycle life that can withstand various mechanical and environmental stresses.[99]

4. Graphene-Based Composites in Sensors and Actuators

4.1. Graphene-Based Sensors

The attractive aforementioned properties of graphene are also desirable in sensing devices, devices that detect changes in the environment and then convert these changes to analyzable signals. Electrons present in graphene's p-orbital form π-bonds with their surrounding atoms, which are highly sensitive to environmental change.[100] Of particular interest to sensors, graphene's high electron mobility, large specific surface area, superior conductivity, and low electrical noise make it an exceptional candidate.[101] While graphene is inherently hydrophobic and brittle, GO and rGO are more hydrophilic and ductile due to the oxygen functional groups present (i.e., hydroxy, epoxy, and carboxyl groups).[10]

4.1.1. Chemical and Biosensors Sensors

Graphene in its original structure is chemically inert, thus for chemical sensors, pristine graphene is either doped or utilized as a dopant.[100] Alternatively, GOs and rGOs lack this chemical barrier and can be utilized as they are. In sensing gases such as carbon dioxide (CO_2), ammonia (NH_3), hydrogen sulfide (H_2S), nitrogen dioxide (NO_2), ethanol (C_2H_5OH), and sulfur hexafluoride (SF_6) decomposition products, graphene nanosheets is the most common form of graphene used due to its porous nature.[102,103] For example, Bai et al. modified copper oxide (CuO) nanoflakes with rGO nanosheets, which resulted in an ultrafast responsive NO_2 (5 ppm) gas sensor at low detection limits, all whilst under room temperature.[104] The CuO/rGO sensors exhibited NO_2 response rates of 400.8% and 20.6% for 5 ppm and 50 ppb, respectively. With the 5 ppm response time being as rapid as 6.8 s at 23 °C. It is worth mentioning that GO is electrically insulating due to the numerous pendant oxygen groups, hence, rGO (with its chemically active defect sites) is more promising, especially in conductance-based sensors.[101]

Graphene-based biosensors are actively being developed to detect RNA and DNA strands. Feng et al. sought to enhance their titanium nitrate (TiN) electrochemical sensor for detecting dopamine (DA), uric acid (UA), and ascorbic acid (AA) simultaneously and distinctively.[105] These biomolecules coexist naturally in the human body, however, abnormal concentrations of them are related to conditions such as schizophrenia, Parkinson's disease, hyperuricemia, gout, or kidney stones.[105,106] Their previous TiN-only sensor achieved detection limits of 1.2 µM for DA and 1.5 µM for UA.[107] However, when incorporating rGO to produce TiN-rGO composites, the detection limits were remarkably lowered to 0.11 µM for DA and 0.12 µM for UA; with extended linear ranges of 0.5–210 µM for DA and 5–350 µM for UA. The improvements were achieved with no disruption to the original TiN structure. RGO has displayed enhanced sensitivity, conductivity, and surface area while reducing noise and interference. The resultant TiN-rGO composite offers a highly effective sensor for precise and broad detection.

The most recent global pandemic, SARS-CoV-II (COVID19), was a catalyst for scientists to tackle the topic from various fields. Early diagnosis was proven to improve prognosis,[108] thus, the detection of SARS-CoV-II virus RNA strains and antibodies was of high interest amongst the sensors community. Seo et al. developed a field-effect transistor (FET) biosensor by conjugating a graphene sheet with SARS-CoV-II spike antibody.[109] The graphene's high conductivity and surface sensitivity

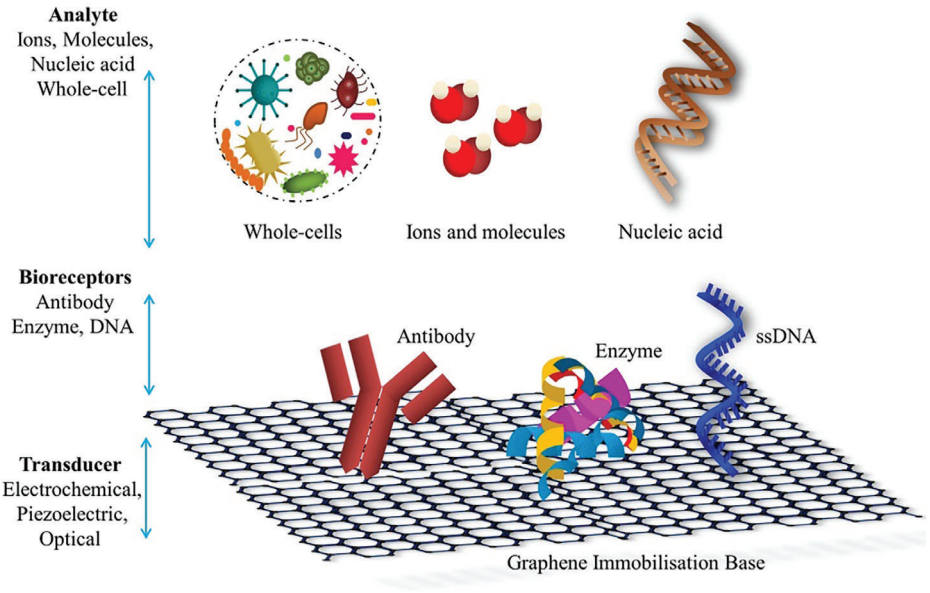

Figure 16. Schematic illustration of graphene-based biosensors where antibodies, enzymes, and ssDNA are immobilized on the surface of the graphene which acts as bioreceptors for target analytes like whole cells, ions/molecules, and nuclei acid. Reproduced with permission.[112] Copyright 2020, Elsevier.

facilitated a detection limit of 1 fg mL^{-1} in phosphate-buffered saline and 100 fg mL^{-1} in a clinical transport medium. This functionalization of the graphene sheet enabled rapid detection of the virus in human nasopharyngeal swab specimens. Ali et al. utilized aerosol jet nanoprinting to create 3D electrodes coated with rGO.[110] During fabrication, SARS-CoV-II antigens were successfully bonded with rGO nanoflakes. The rGO coating provided enhanced electron transport and a large surface area, enabling the sensor to achieve an ultrasensitive detection limit of 2.8×10^{-15} M in just seconds. Likewise, graphene could also be employed in DNA sensing. Mohanraj et al. synthesized conductive ink from exfoliated graphene, which was then utilized to fabricate paper-based electrodes.[111] In addition to its large surface area, the paper-based graphene enabled greater immobilization of DNA probes and improved interaction with target analytes. In addition to it being affordable, biocompatible, and disposable. Rapid and direct electrochemical analysis was achieved without extensive sample preparation highlighting graphene's versatility and pivotal role in advancing practical, efficient, and reliable sensing technologies. **Figure 16** summarizes graphene applications in biosensing.

4.1.2. Physical Sensors and Actuators

The versatility of graphene-based composites, attributed to their biocompatibility, flexibility, lightweight nature, and previously mentioned properties, fulfills the essential performance requirements for physical sensors (e.g., pressure, strain, and temperature sensors) as well as actuators (electrothermal, electrostatic, and ionic actuators) (**Figure 17**). Hence, graphene-based composites are emerging candidates in stretchable wearable technologies, human-machine interfaces, soft robotics, health monitoring, etc.[113] Human skin is ductile enough to strain beyond 50%, while conventional strain sensors suffer from low-strain resolution (less than 5%).[114] Another limitation of conventional strain sensors is their low sensitivity or gauge factor (GF), defined as the ratio between the relative change in electrical resistance to the mechanical strain.[115] Thus, a good strain sensor exhibits a high gauge factor that amplifies the effect of low strains, while also preserving its mechanical integrity and responsiveness at high strains. Nuthalapati et al. synthesized a novel palladium (Pd) and rGO nanocomposite.[114] The rGO-Pd nanosensor was tested over a large range of strains, 0.1—45%. Remarkable GF values were achieved across different strains, namely, 14, 89, 177, and 1523 for 0.1%, 0.5%, 20%, and 45% strains, respectively. In addition to a rapid response time of 47 ms, that demonstrates the capability of sensing a wide range of activities: from real-time pulse monitoring to physical finger and hand movement. In their pursuit to mimic the mechanical pressure receptors of human skin (ranging from ≈1 Pa to 300 kPa), Cao et al. resorted to graphene as their piezoresistive pressure sensor.[116] Fabrication was followed through using 3D printing of laminated pristine graphene layers. The sensor demonstrated a wide detection range, from a low detection limit of 1 Pa and up to 400 kPa, that exceeded human skin's upper range. High sensitivities were also found to be 3.1 kPa^{-1} for pressures between 1 Pa and 13 kPa, and 0.22 kPa^{-1} for pressures between 13 and 400 kPa.

Smart actuators are often inspired by the natural environment-responsive nature. Janus materials are characterized as engineered materials with two (or more) disparate constituents, with differing physical or chemical properties that result in an anisotropic behavior. Che et al., laminated rGO layers onto cellulose nano paper (CNP) using lignin as a natural adhesive to mimic the reversible movement of pinecones.[117] rGO promoted hydrophobicity, electrical conductivity, and thermal stability, while CNP provided a flexible, lightweight, and hydrophilic

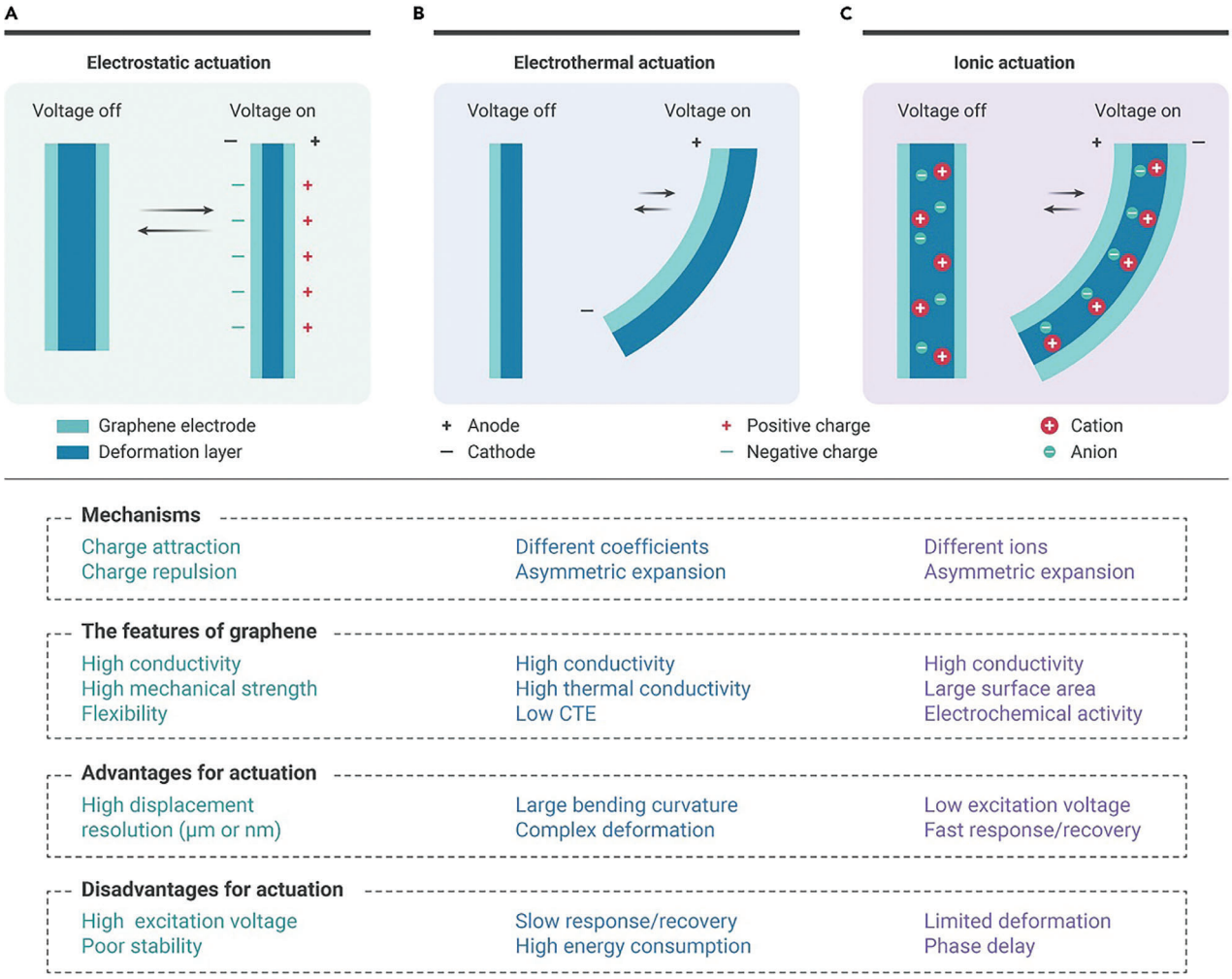

Figure 17. Schematic illustration summarising the mechanisms, features of graphene, advantages, and disadvantages for ERAs based on graphene; a) Electrostatic actuators, b) electrothermal actuators, and c) ionic actuators. Reproduced with permission.[120] Copyright 2021, Elsevier.

support structure. The rGO/CNP Janus film achieved a fast response speed to electrical stimuli (compared to other carbon/polymer bilayers of comparable weight),[118,119] with a value of 1.875 s^{-1} V^{-1} response speed. Moreover, the film maintained actuation performance over 1000 cycles, which is noteworthy given that mechanical integrity across cyclic actuation is essential.

4.2. Graphene-Based Hydrogels and Aerogels

Hydrogels are crosslinked polymeric networks with high flexibility and biocompatibility commonly used in drug delivery, wound dressing, and agricultural nutrient transfer.[121] Due to the hydrophilic nature of their backbone and/or side chains, they are exemplary superabsorbents. Hydrogels are capable of absorbing, retaining, and desorbing large amounts of water; up to 100000 times their dry mass or 99.9 wt.% without dissolving or losing structural integrity.[121–124] Hence, rendering them ideal biomimicry platforms. When the liquid phase in a hydrogel is replaced with air, the resultant is a rigid, highly porous, lightweight structure—known as aerogel. Aerogels are valued for their ultralow densities, high surface area, and thermal insulation. Both hydrogels and aerogels could be synthesized from natural or synthetic polymers, or a blend of both. Natural polysaccharides (e.g., cellulose, chitosan, hemicelluloses) are common hydro/aerogel backbones, thus, they will be focused on herein.

Mittal et al. used GO nanosheets as a chitosan and carboxymethyl cellulose (CMC) crosslinker to synthesize dye-contaminated wastewater treatment hydrogels.[125] The hydrogel benefited from GO's mechanical properties, thermal stability, and adsorption efficiency; chitosan's adsorption capacity and biocompatibility; and CMC's water solubility and binding properties. Nearly 99% and 82% of the dye were absorbed from a methyl blue dye solution and a methyl orange solution, respectively. Adsorption thermodynamics were spontaneous, and the hydrogels maintained their high adsorption efficiencies over 20 adsorption-desorption cycles.

In their pursuit to produce polymer-based efficient electromagnetic interference (EMI) shielding and thermal management

materials, Song et al. fabricated flexible cellulose-derived carbon aerogels reinforced with rGO and backfilled with polydimethylsiloxane (PDMS).[126] The cellulose/rGO/PDMS aerogels demonstrated a shielding effectiveness of 51 dB, which is comparable to metals but with significantly reduced weight. Additionally, the aerogels exhibited excellent thermal stability and mechanical properties, with a 178.3 °C heat-resistance index, a thermal conductivity of 0.65 Wm^{-1} K^{-1}, tensile strength of 4.1 MPa, and a value of 42 on a durometer scale (Shore A hardness).

5. Graphene-Based Materials for Water Treatment

Water is undoubtedly the most valuable resource on our planet, crucial for the survival of humankind. The constant increase in water consumption and the acceleration of water-polluting activities worldwide make preserving scarce water resources one of the urgent challenges for the global community. Industrial, domestic, and agricultural wastewater contain significant amounts of hazardous organic and inorganic pollutants that pose a severe environmental threat to both the natural environment and living beings.[127] The combination of desirable chemical properties, wide surface area, high selectivity, outstanding mechanical properties, and relatively low cost makes the application of nanomaterials, particularly graphene-based nanostructures, especially promising in wastewater treatment and purification processes.

Many methods are available for modifying graphene and graphene-based materials, opening up several opportunities for water treatment, purification, separation, desalination, and disinfection.[128] The four primary water treatment methods for graphene and its derivatives include membrane-based techniques, photocatalytic oxidation, adsorption, and electrochemical oxidation. A high surface-to-weight ratio of ≈2600m^2g^{-1} qualifies graphene-based materials to be an effective adsorbent in eliminating both heavy metal ions and organic molecules from industrial effluents.[129]

Due to its inherent hydrophobicity, pristine graphene cannot be effectively dispersed in aqueous solutions. This inevitably imposes certain limitations on its application in the field of water treatment. Chemically converted graphene systems, namely reduced rGO and GO, are widely regarded as the most attractive derivatives for use in water purification systems.[130] The presence of multiple oxygen-containing functional groups (carboxyl, epoxide, hydroxyl, carbonyl) in GO imparts a high negative charge density and hydrophilic nature to the surface, making the material the most widely employed graphene compound in water treatment.[131] A high-water cleanup efficacy of rGO toward metal ions and anionic dyes is due to the lack of negative charge on the graphene surface. In recent years, various graphene-based composites have been explored to enhance the performance of this class of nanomaterials in terms of photocatalytic, photoelectrocatalytic, catalytic, and electrocatalytic activity, adsorption capacity, and desalination ability in various water treatment settings.[130]

5.1. Water Treatment Methods

5.1.1. Adsorption

Adsorption is a well-established and highly efficient wastewater treatment method due to the simplicity of apparatus design, ease of operation, and convenience. This process is often the preferred option for removing dissolved pollutants left after chemical and biological oxidation treatments. Graphene and its derivatives have successfully demonstrated high adsorption efficiency for such types of contaminants as organic dyes, heavy metal ions, and halomethanes.[132–136] The use of GO as an adsorbent is accompanied by a challenging process of separating this compound from the water after adsorption due to the high stability of its dispersion in the water and high hydrophilicity. In recent years, the magnetization of graphene-based adsorbents has been investigated as a potential solution to this problem. The combination of GO as an adsorbent and a material exhibiting magnetic properties (e.g., Fe_3O_4) makes it possible to magnetically separate the reacted adsorbent from the treated water.[137,138]

The literature reports the use of graphene nanosheets as highly effective adsorbents of a broad range of organic compounds, namely halogenated aliphatic, plasticizers, polycyclic aromatic hydrocarbons, dyestuff, pharmaceuticals, pesticides, polychlorinated biphenyls, and dyes.[133] Meanwhile, various hybrid composites, including GO-calcium alginate,[139] chitin/GO gels,[140] and rhamnolipid-functionalized graphene,[141] are suitable absorbers of various dyes.[142]

5.1.2. Photocatalysis

Photocatalytic oxidation of contaminants in water and wastewater is a relatively new and growing technological approach in industrial wastewater systems. The principle of operation of a photocatalyst is based on the excitation of the electrons of the valence band to the conduction band to generate electron-hole pairs at sufficient photo energy. The resultant photo-induced carriers initiate a chain of oxidation and reduction reactions, generating additional active species that facilitate the photocatalytic degradation of pollutants.[131] Graphene-based materials are attractive candidates to be used in the preparation of novel composite photocatalysts due to their superior chemical stability across a broad pH range, tunable chemical and structural properties, and remarkable electronic characteristics.[143,144]

In composite photocatalytic systems composed of graphene material and metal oxide, the outstanding contaminant degradation efficiency can be explained by the combined effect of ionic interactions between oxygen-containing functional groups on the surface of graphene-based material and organic pollutants and the increased surface area attributed to the presence of graphene nanosheets. In addition, graphene acts as a photosensitizer, electron acceptor, and adsorbent, accelerating the photodecomposition of contaminants.[145] Recent studies have suggested that the use of 3D graphene-based gels can significantly improve the photocatalytic performance of hybrid materials, as well as make the material more convenient to work with. A study by Zhang et al. concluded that the hierarchical porous scaffold of 3D graphene has a noticeably large surface area, thus positively affecting the adsorptive capacity of the material.[146]

5.1.3. Membrane Filtration

Over the decades, membrane technology has proven itself as a highly efficient and reliable approach for water treatment and

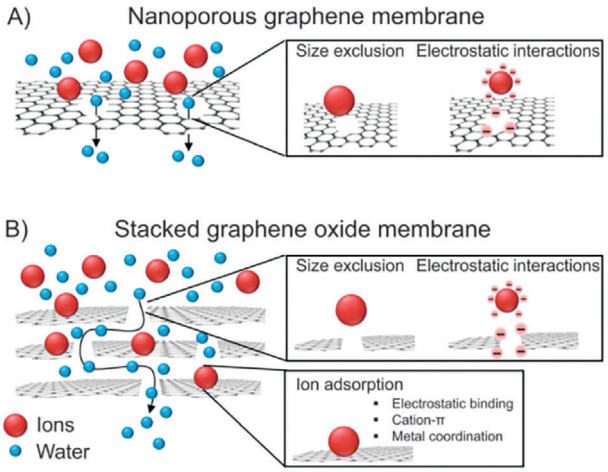

Figure 18. Types of graphene-based membranes: nanoporous graphene a) and stacked GO membranes b). Reproduced with permission.[150] Copyright 2021, Elsevier Ltd.

filtration. Purification of water and wastewater using membrane-based technologies is expected to play a central role in fields such as desalination of seawater, wastewater reuse, and drinking water treatment. The applicability of this technological approach to sustainable industrial designs is mainly due to the ease of operation, low energy consumption, lower space requirements, lack of chemical additives, lack of phase changes, and ease of scaling. Polymeric membranes, the most widely used membrane type in water purification processes, have some notable shortcomings that limit their application in industrial settings. In particular, conventional membranes are often characterized by insufficient mechanical strength, high fouling tendency, low flux, and high hydrophobicity.[131]

Graphene-based membranes demonstrate striking mass-transport and molecular separation properties, as well as outstanding resistance to fouling that cannot be found in any other commercial membranes currently on the market.[147] Moreover, membranes based on GO exhibit exceptional permeability properties, opening up new opportunities for developing highly selective and ultra-fast processes for transporting gas and water molecules through the membrane.[148] There are three methods for modifying graphene-based membranes: direct perforation of the surface to obtain particle screening performance, the embedding of polymer layers between GO sheets, and the introduction of additional functional groups to pristine graphene or GO.[128,149] **Figure 18** shows two common types of graphene-based membranes.

Nanoporous graphene-based membranes are specifically designed to ensure that larger volumes of water can pass through continuous channels at a much lower pressure than is required for conventional polymer membranes. Today, precise control of channel pore size remains one of the challenges. The delocalized π-orbital electron clouds effectively block the gap in the graphene atomic rings, limiting the passage of the smallest molecules.[151] Three main mechanisms of separation of contaminants in graphene-based membranes are size exclusion, adsorption, and Donnan exclusion.[152]

Inkjet printing has emerged as a cost-effective, fast, and scalable technology for applying uniform ultrathin layers (from 7.5 to 60 µm) of graphene-based filtration membranes on polymeric substrates. Fathizadeh et al.[153]reported that printed GO membranes demonstrated an over 95% rejection of small organic molecules and about one order of magnitude greater water permeance compared to commercially available polymeric membranes. These membranes also demonstrated outstanding efficiency (a rejection rate of ≈95%) in removing pharmaceutical contaminants.

5.1.4. Electrochemical Purification

Electrochemical methods have received considerable attention as water treatment techniques due to their environmental compatibility without sacrificing high efficiency.[131] Advanced processes of electrochemical oxidation, including solar photo-electro-Fenton, anodic oxidation, and electro-Fenton, were adapted for the effective elimination of harmful contaminants.[154] The use of graphene-based materials as suitable capacitive deionization electrodes in electrochemical processes has great prospects due to commercial availability, high stability, excellent conductivity, and non-toxicity of this class of materials.[131] Mousset et al. investigated the potential of different forms of graphene electrodes (single-layer graphene, multilayer graphene, graphene foam) for the electro-Fenton purification of wastewater. The authors reported that all the studied materials can successfully produce H_2O_2 by Fe^{2+} regeneration, form OH via the Fenton reaction, and efficiently degrade phenol.[155]

5.2. Application Fields of Graphene-Based Materials

5.2.1. Removal of Organic Contaminants

A broad range of organic pollutants can be present in industrial, agricultural, and domestic wastewaters, such as oils, pesticides, dyes, hydrocarbons, herbicides, polycyclic aromatic hydrocarbons (PAHs), proteins, fertilizers, greases, pharmaceuticals, and carbohydrates. GO and related composite materials have been thoroughly explored as a highly efficient and sustainable alternative to conventional organic adsorbents.[142] The efficiency of the removal process from water directly depends on several properties of organic pollutants, including the geometry and size of the molecule, the presence of different functional groups, hydrophobicity, and aromaticity. Polar or hydrophobic organic contaminants demonstrate compatibility with pristine graphene, whereas their basic, acidic, or ionic counterparts are compatible with the electrically charged surface of GO.[156] In addition, various properties of the background solution (e.g., temperature, the pH level, the presence of natural organic matter, ionic strength) have a significant influence on the treatment of wastewater by affecting the physical and chemical interactions between organic pollutants and graphene-based compounds used as adsorbents.

Dyes are the emerging class of organic pollutants that encompasses a broad range of natural and synthetic substances. In recent years, the relatively high efficiency of GO in the removal of several major dye compounds, in particular rhodamine

B, methyl blue, methyl orange, methyl green, and basic red 12, has been reported.[157] An endothermic adsorption process accompanies the treatment of water contaminated by dye pollutants with GO. An increase in the degree of oxidation of the surface of GO leads to a more efficient removal of dye molecules from the aqueous phase. A negative charge imparted by the oxygen functionalities to the surface of GO promotes the adsorption of cationic dyes due to the electrostatic charge.[158] Several GO composite systems, including polymer/GO, hydrogel/GO, magnetic graphene/GO, and poly(m-phenyleneisophthalamide)/GO, have found practical applications in wastewater treatment systems for dye adsorption.[159]

Pharmaceutical contaminants (e.g., endocrine-disrupting chemicals, antibiotics) constitute another broad class of organic pollutants where both pristine graphene and GO demonstrate high efficiency as adsorbents. A single-layered carbon structure of graphene means that all carbon atoms can easily contact antibiotics via π–π interaction. Moreover, the high surface area and porous structure of graphene-based materials facilitate faster diffusion and surface reactions of antimicrobial substances, allowing them to achieve rapid adsorption.[160,161] Various graphene-based composites have been studied for the removal of pharmaceutical contaminants. Li et al. investigated the potential of the RGO/Bi_2WO_6 systems in the removal of ciprofloxacin hydrochloride under simulated visible light.[162]

One of the currently unsolved critical issues in water treatment is the sustainable separation of oil in water emulsion due to the colossal volume of oily wastewater accompanying various industrial operations. Alammar et al. investigated the performance of graphene-based nanocomposite membranes for oil-in-water emulsion separation.[163] The authors noted that in addition to sufficient antimicrobial and antifouling properties, these membranes demonstrate an outstanding oil-removal efficiency of up to 99.9%. This effect is achieved by introducing only a few wt.% GO into the polybenzimidazole matrix. The application of GO membranes in industrial water treatment is extremely promising because of the outstanding productivity rate, long-term stability, and high selectivity of the separation process.[164]

5.2.2. Removal of Inorganic Contaminants

In recent years, graphene-based materials have attracted considerable interest as advanced adsorbents for the removal of rare earth and heavy metal ions from wastewater due to the combination of fast kinetics, high contaminant removal efficiency, and strong affinity to a wide range of metal ions.[165] Heavy metals, which raise serious concerns in terms of clean water supply, belong to the group of trace elements with an elemental density exceeding $4 \pm 1 g\,cm^{-3}$. The metal and metalloids with the most hazardous environmental potential are Pb, Cd, Hg, Cr, and As.[127] The effective removal of these contaminants directly depends on the following factors: the presence of background ions, the pH level of the environment, the presence of natural organic matter, and the temperature of wastewater.[166] The endothermic nature of the process of adsorption of inorganic pollutants makes wastewater treatment systems based on GO or graphene composites particularly attractive.

Graphene derivatives have demonstrated sufficient efficiency as adsorbents for the removal of Fe^{+2} and Co^{+2} ions from contaminated water.[167,168] A study by Ain et al. highlighted the potential of magnetic GO fabricated via the co-precipitation method for removing Pb^{+2}, Cu^{+2}, Ni^{+2}, Cr^{+3}, and Zn^{+2} ions from aqueous solution. The studied graphene systems demonstrated good reusability, as evidenced by experimental data (the total absorption capacity in the range of 87.51%–78.12%) after four successive adsorption–desorption cycles.[137]

Most of the research on incorporating graphene-based water treatment systems for the removal of rare earth metal ions has focused on GO due to the presence of various oxygen-containing groups and the charged surface. This graphene derivative shows high efficiency as an adsorbent to remove ions of La, Y, Gd, and Nd from contaminated aqueous solutions. GO functionalized with $Ti_3(PO_4)_4$ and Fe_3O_4 and GO-polyaniline nanocomposites are promising candidates for these applications.[166] Zong et al. reported that magnetic graphene/iron oxide composite (Fe_3O_4/GO) exhibited the strong points of both GO nanomaterials and iron oxide and demonstrated excellent adsorption potential in removing radionuclides.[169] The maximum sorption capacity of U^{6+} ions on the studied composite was 69.49 mg g^{-1}, which is higher than the values reported for the majority of nanomaterials of other classes.

Desalination is the emerging approach to supply additional volumes of clean water in the context of a growing global water scarcity.[170,171] Thermally rGO membranes are gaining increased attention in the membrane separation field for use in industrial-scale desalination processes. Li et al. reported that the introduction of plane nanopores into GO nanosheets by the method of H_2O_2 oxidation allowed achieving a sharp increase in water permeability of the membrane without a noticeable drop in the membrane selectivity in terms of Na_2SO_4 separation.[172] Tailored graphene membranes have demonstrated high efficiency in removing salts typical of seawater, including KCl, $MgCl_2$, NaCl, and $MgSO_4$.[130]

5.2.3. Water Disinfection

Various graphene-based materials, including metal oxide incorporated with GO or rGO, GO films, GO membranes, graphene nanowalls, and graphene nanorods, are well suited for use in water disinfection systems. The degradation or inactivation of microbes, bacilli, and other types of microorganisms by graphene-based systems occurs through either photo light-induced degradation as demonstrated in **Figure 19** using graphene-ZnO photocatalyst, or the breaking of the bacterial cell wall by direct contact.[130] Recent studies have confirmed the excellent antimicrobial properties of graphene-based materials against such microorganisms as *Staphylococcus aureus*, *Escherichia coli*, *Bacillus subtilis*, *Yersinia bacteria*, and *Pantoea agglomerans*. The maximum removal efficiencies of magnetic GO toward Yersinia bacteria, *E. coli*, and *Pantoea agglomerans* were reported to be 97.2%, 98.8%, and 97.7%, respectively.[137]

As mentioned, chemical oxidation and physical disruption are the two main mechanisms behind the antimicrobial activity of graphene. Physical disruption also referred to as mechano-bactericidal activity, is associated with the loss of membrane

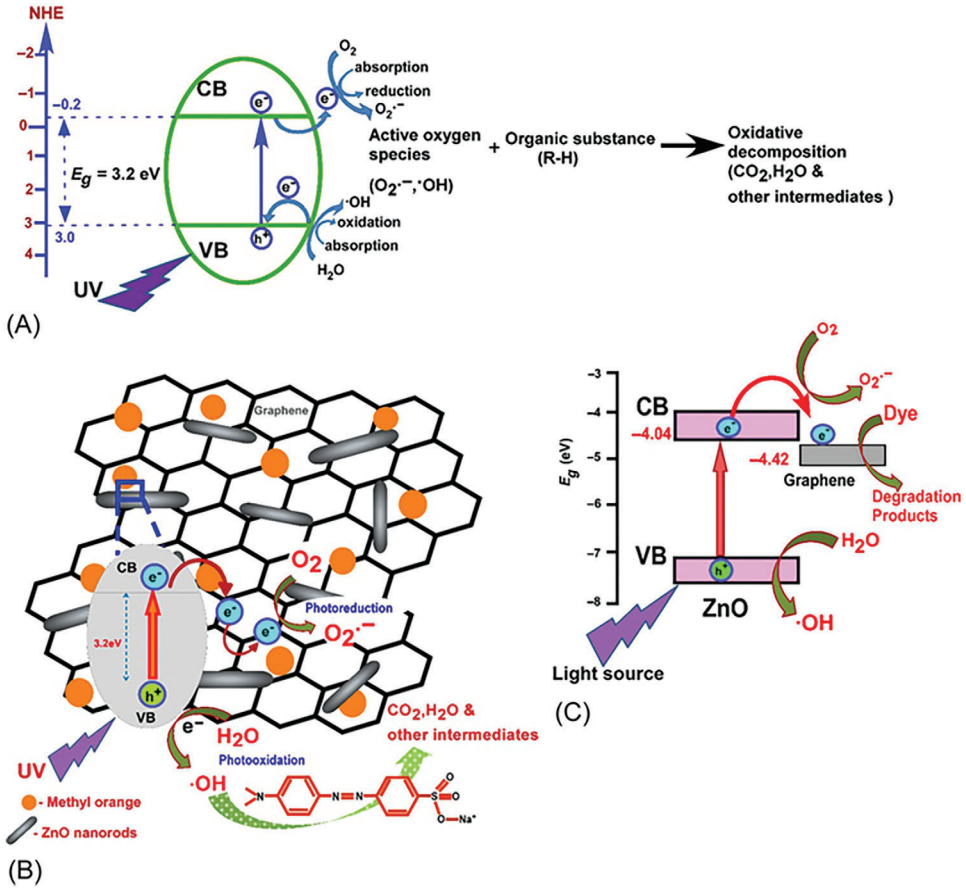

Figure 19. Schematic illustration of the photocatalytic mechanism of a) ZnO photocatalyst and b) graphene-ZnO photocatalyst, c) band diagram for graphene-ZnO. Reproduced with permission.[131] Copyright 2019, Elsevier.

integrity as a result of the penetration of atomically sharp edges of graphene nanosheets into the cell membrane. In the case of chemical oxidation, nanosheets of GO mediate oxidative stress on the cellular components or cell structure through the direct transfer of electrons or via the generation of reactive oxygen species.[173]

6. Conclusion and Future Direction

In conclusion, the wide range of graphene's applications is huge and still growing, with ongoing research continuously exploring new opportunities and surpassing challenges. Graphene's unique set of properties not only promises to enhance existing technologies but also paves the way for innovations to improve technologies and enhance the quality of life.

Different types of graphene materials have been reported to improve the thermal and mechanical properties of polymers of different nature. However, in order to maximize its potential, effectively transfer the outstanding properties of graphene from the nanoscale to the macroscale, and achieve important levels of reinforcement, an effective stress transfer between graphene and polymer is vital. For that, lengths ≥20 μm are required for unfunctionalized graphene or a rational chemical functionalization (e.g., grafting graphene with strategically selected polymer chains) needs to be designed to achieve good levels of reinforcement as well as improved thermal properties through enhanced compatibilities, which lead to improved dispersions of graphene in the host matrix and stronger graphene-polymer interfaces.

The horizon for graphene in energy storage applications is very promising, this is a herald of better days to come when the energy systems will be more efficient, stronger, and capable enough to stand up to ever-increasing technological needs and demands for sustainable energy. Various forms of energy storage were discussed, and it was shown how graphene has great potential for use in the field of energy storage because it has unmatched electrical conductivity, high mechanical strength, and a very large surface area that has a promising perspective as far as development of advanced batteries and supercapacitors are concerned. These graphene-improved energy storage solutions promise not only to reduce charging time by a huge margin but also to increase energy density while extending the devices' lifetime; this makes them key for mass adoption of electric vehicles, integration with renewable sources of power, and portable electronic equipment evolution. This paves the way for scaling up and integrating research which in turn clears the path for graphene's central role in the next generation of electrochemical energy storage technologies aimed at ultimately contributing toward an overall more efficient and greener future.

Graphene's exceptional conductivity, surface area, and tunable properties have proven promising in advancing sensor and

actuator technologies. Its biocompatibility and non-toxicity enable it as a top candidate for biomedical, wearable technologies, soft robotics, and agricultural applications. The reviewed literature highlighted the transformative impact of graphene and its derivatives across the chemical, biosensing, physical sensing, and actuating technologies, evidently reporting unprecedented detection limits, response times, and extended operational/cyclical performances.

Furthermore, the implementation of graphene in water treatment was reviewed, which demonstrates that investigating and using graphene for water treatment can be revolutionary in terms of more efficient, more effective, and greener purification technologies. Graphene's exceptional properties, such as its high surface area, permeability to water molecules, and ability to adsorb a wide range of contaminants, from heavy metals to organic compounds and bacteria, position it as a transformative material in the field of water purification. Looking forward, the focus will increasingly be on overcoming current challenges related to the scalable production of graphene and its composites, enhancing its selectivity and reusability, and integrating these advanced materials into existing water treatment infrastructures. Graphene-based membranes, adsorbents, and catalytic systems that are new, creative, and emerging will have a significant impact on the global quest for making water clean hence contributing toward the sustainability of water resources and lessening environmental harm that comes with water treatment processes. The potential of graphene to transform water treatment is becoming more apparent as research continues forward; one day we may have a world where access to clean and safe drinking water is easier and sustainable.

Moreover, it is believed that future research should also focus on implementing machine learning (ML) and artificial intelligence (AI) to accelerate the discovery, optimization, and characterization of graphene-based composites, enabling predictive, data-driven innovation across nanotechnology and materials engineering. The combination of machine learning and artificial intelligence in graphene-based nanocomposite studies has the potential to transform material exploration, improvement, and analysis. AI-driven predictive models enable rapid identification of material properties, while data-driven design uncovers novel composite configurations tailored for specific applications. Advanced image analysis techniques automate structural characterization, and ML optimizes manufacturing processes for enhanced scalability and quality. AI bridges multi-scale interactions from quantum to macroscopic levels supports sustainable development through lifecycle analysis, and accelerates the discovery of multi-functional composites. Furthermore, recent advancements have demonstrated the application of ML and AI in optimizing the properties of GO-based membranes, enabling precise control over structural parameters and performance. These methods allow efficient prediction and fine-tuning of membrane characteristics, such as pH and ionic strength, to optimize performance. For example, AI-driven approaches have been successfully employed to enhance material design for membrane technologies.[174] In another recent study, a set of crucial parameters (such as GO layer thickness, roughness, zeta potential, and water contact angle) were benchmarked to gather relevant experimental data from the literature, which were then utilized to develop algorithms for predictions of the effect of GO membrane microstructure on its performance.[175] Machine learning has shown promise in predicting graphene defects. A novel approach was introduced by Zheng and Gu to identify defects in graphene sheets by analyzing their thermal vibrational topographies.[176] Two strategies were developed: an atom-based method and a domain-based method. The former constructs data from atom indices, while the latter is by domain discretization. Both methods, while non-destructive and offering atomic precision, achieved a remarkable prediction accuracy of ≈90% on reserved testing data. This provides a highly accurate, non-destructive, and less technically demanding alternative to traditional transmission electron microscopy techniques.

Finally, the range of graphene applications varies from creating strong composites to modifying and enhancing energy storage technologies in addition to innovative water filtration and treatment methods. However, the key to achieving the desired goal of implementing graphene and making the most of its remarkable properties is in the combined endeavors of the research communities, industries, and policymakers in surmounting technical, economic, and regulatory barriers. By all means, graphene's journey toward shaping technology and sustainability by using it in different sectors is very promising and it is believed that it will have a positive and direct impact on our daily lives and global economy through the implementation of graphene as well as the continuous efforts toward solving its current challenges.

Conflict of Interest

The authors declare no conflict of interest.

Keywords

actuators, composites, energy storage, graphene, nanomaterials, sensors, water treatment

Received: August 24, 2024
Revised: January 14, 2025
Published online:

[1] A. K. Geim, K. S. Novoselov, *Nat. Mater.* **2007**, *6*, 183.
[2] N. Wang, M. K. Samani, H. Li, L. Dong, Z. Zhang, P. Su, S. Chen, J. Chen, S. Huang, G. Yuan, X. Xu, B. Li, K. Leifer, L. Ye, J. Liu, *Small* **2018**, *14*, e1801346.
[3] F. Bonaccorso, L. Colombo, G. Yu, M. Stoller, V. Tozzini, A. C. Ferrari, R. S. Ruoff, V. Pellegrini, *Science* **2015**, *347*, 1246501.
[4] 15 years of graphene electronics, *Nat. Electron.* **2019**, *2*, 369.
[5] Y. Sun, M. Sun, D. Xie, in *Graphene* (Eds: Z. Xu, D. Xie, Y. Fang), Academic Press, Cambridge, MA, USA **2018**, pp. 103–155, https://doi.org/10.1016/B978-0-12-812651-6.00005-7.
[6] J. Zhao, P. Ji, Y. Li, R. Li, K. Zhang, H. Tian, K. Yu, B. Bian, L. Hao, X. Xiao, W. Griffin, N. Dudeck, R. Moro, L. Ma, W. A. de Heer, *Nature* **2024**, *625*, 60.
[7] Y. Chendake, H. Mhetre, S. Khatavkar, V. Mehtre, S. Namekar, V. Kaduskar, P. Chougule, in *Recent Advances in Graphene Nanophotonics*, Springer Nature, Cham, Switzerland **2023**, pp. 83–118.
[8] X. Yu, H. Cheng, M. Zhang, Y. Zhao, L. Qu, G. Shi, *Nat. Rev. Mater.* **2017**, *2*, 17046.
[9] S. Syama, V. Mohanan, *Int. J. Biol. Macromol.* **2016**, *86*, 546.

[10] X. Wei, L. Mao, R. A. Soler-Crespo, J. T. Paci, J. Huang, S. T. Nguyen, H. D. Espinosa, *Nat. Commun.* **2015**, *6*, 8029.
[11] A. G. Olabi, M. A. Abdelkareem, T. Wilberforce, E. T. Sayed, *Renew. Sustainable Energy Rev.* **2021**, *135*, 110026.
[12] A. K. Tareen, K. Khan, M. Iqbal, Y. Zhang, J. Long, F. Nazeer, A. Mahmood, N. Mahmood, Z. Shi, C. Ma, W. Huan, M. F. Khan, J. Yin, C. Li, H. Zhang, *J. Mater. Chem. C* **2022**, *1*, 11472.
[13] M. K. Kumar, M. Muthuvinayagam, in *Graphene: Fabrication, Properties and Applications* (Eds: R. T. Subramaniam, R. Kasi, S. Bashir, S. Sharma, A. Kumar), Springer Nature, Singapore **2023**, pp. 167–193.
[14] S. Sharma, K. Qanungo, *AIP Conf. Proc.* **2023**, *2535*, 030012.
[15] P. Bhol, S. Yadav, A. Altaee, M. Saxena, K. Misra, A. K. Samal, *ACS Appl. Nano Mater.* **2021**, *4*, 3274.
[16] Y. Dai, M. Liu, J. Li, N. Kang, A. Ahmed, Y. Zong, J. Tu, Y. Chen, Zhang, X. Liu, *Polymers* **2022**, *14*, 4246.
[17] L. Zhu, X. Guo, Y. Chen, Z. Chen, Y. Lan, Y. Hong, W. Lan, *ACS Appl. Nano Mater.* **2022**, *5*, 3643.
[18] S. Khaliha, A. Bianchi, A. Kovtun, F. Tunioli, A. Boschi, M. Zambianchi, D. Paci, L. Bocchi, S. Valsecchi, S. Polesello, A. Liscio, M. Bergamini, M. Brunetti, M. Luisa Navacchia, V. Palermo, M. Melucci, *Sep. Purif. Technol.* **2022**, *300*, 121826.
[19] L. Gong, I. A. Kinloch, R. J. Young, I. Riaz, R. Jalil, K. S. Novoselov, *Adv. Mater.* **2010**, *22*, 2694.
[20] S. Chatterjee, F. Nafezarefi, N. H. Tai, L. Schlagenhauf, F. A. Nüesch, B. T. T. Chu, *Carbon* **2012**, *50*, 5380.
[21] L. Zhu, F. Scheiba, V. Trouillet, M. Georgian, Q. Fu, A. Sarapulpva, F. Sigel, W. Hua, H. Ehrenberg, *ACS Appl. Energy Mater.* **2019**, *2*, 7121.
[22] P. May, U. Khan, A. O'Neill, J. N. Coleman, *J. Mater. Chem.* **2012**, *22*, 1278.
[23] C. Vallés, A. M. Abdelkader, R. J. Young, I. A. Kinloch, *Compos. Sci. Technol.* **2015**, *111*, 17.
[24] C. Vallés, A. M. Abdelkader, R. J. Young, I. A. Kinloch, *Faraday Discuss.* **2014**, *173*, 379.
[25] J. P. Rourke, A. Pandey, J. J. Moore, M. Bates, I. A. Kinloch, R. J. Young, N. R. Wilson, *Angew. Chem. Int. Ed. Engl.* **2011**, *50*, 3173.
[26] H. R. Thomas, S. Day, W. E. Woodruff, C. Vallés, R. J. Young, I. A. Kinloch, G. W. Morley, J. V. Hanna, N. R. Wilson, J. Rourke, *Chem. Mater.* **2013**, *25*, 3580.
[27] H. R. Thomas, C. Vallés, R. J. Young, I. A. Kinloch, N. R. Wilson, J. Rourke, *J. Mater. Chem. C* **2013**, *1*, 338.
[28] D. Li, M. B. Müller, S. Gilje, R. B. Kaner, G. G. Wallace, *Nat. Nanotechnol.* **2008**, *3*, 101.
[29] C. Vallés, I. A. Kinloch, R. J. Young, N. R. Wilson, J. Rourke, *Compos. Sci. Technol.* **2013**, *88*, 158.
[30] X. Liu, L. Li, Z. Chen, X. Duan, Y. Yu, L. Sun, *High Perform. Polym.* **2019**, *32*, 631.
[31] O.-K. Park, M. G. Hahm, S. Lee, H.-I. Joh, S.-I. Na, R. Vajtai, J. H. Lee, B.-C. Ku, M. Ajayan, *Nano Lett.* **2012**, *12*, 1789.
[32] H. R. Pant, Pokharel, M. K. Joshi, S. Adhikari, H. J. Kim, C. H. Park, C. S. Kim, *Chem. Eng. J.* **2015**, *270*, 336.
[33] A. C. Balazs, T. Emrick, T. Russell, *Science* **2006**, *314*, 1107.
[34] L.-Z. Guan, Y.-J. Wan, L.-X. Gong, D. Yan, L.-C. Tang, L.-B. Wu, J.-X. Jiang, G.-Q. Lai, *J. Mater. Chem. A* **2014**, *2*, 15058.
[35] M. A. Gimenes Benega, W. M. Silva, M. C. Schnitzler, R. J. Espanhol Andrade, H. Ribeiro, *Polym. Test.* **2021**, *98*, 107180.
[36] L. Nguyên, S.-M. Choi, D.-H. Kim, N.-K. Kong, P-J. Jung, S.-Y. Park, *Macromol. Res.* **2014**, *22*, 257.
[37] J. Wang, Z. Shi, Y. Ge, Y. Wang, J. Fan, J. Yin, *Mater. Chem. Phys.* **2012**, *136*, 43.
[38] L.-X. Gong, Y.-B. Pei, Q.-Y. Han, L. Zhao, L.-B. Wu, J.-X. Jiang, L.-C. Tang, *Compos. Sci. Technol.* **2016**, *134*, 144.
[39] G. Gonçalves, A. A. Marques, A. Barros-Timmons, I. Bdkin, M. K. Singh, N. Emami, J. Grácio, *J. Mater. Chem.* **2010**, *20*, 9927.
[40] G. P. Kar, S. Biswas, S. Bose, *Phys. Chem. Chem. Phys.* **2015**, *17*, 14856.
[41] S. Guanhong, in *Proc. of China SAE Congress 2021: Selected Papers*, Springer, Singapore **2023**.
[42] C. Vallés, D. G. Papageorgiou, F. Lin, Z. Li, B. F. Spencer, R. J. Young, I. A. Kinloch, *Carbon* **2020**, *157*, 750.
[43] S. Srivastava, N. A. Kotov, in *Semiconductor Nanocrystal Quantum Dots: Synthesis, Assembly, Spectroscopy and Applications* (Ed: A. L. Rogach), Springer Vienna, Vienna **2008**, pp. 197–216.
[44] P. Podsiadlo, B. S. Shim, N. A. Kotov, *Coord. Chem. Rev.* **2009**, *253*, 2835.
[45] P. Podsiadlo, M. Michel, J. Lee, E. Verploegen, N. W. Shi Kam, V. Ball, J. Lee, Y. Qi, A. J. Hart, T. Hammond, N. A. Kotov, *Nano Lett.* **2008**, *8*, 1762.
[46] K. W. Putz, O. C. Compton, M. J. Palmeri, S. T. Nguyen, L. C. Brinson, *Adv. Funct. Mater.* **2010**, *20*, 3322.
[47] K. W. Putz, O. C. Compton, C. Segar, Z. An, S. T. Nguyen, L. C. Brinson, *ACS Nano* **2011**, *5*, 6601.
[48] X. Tian, L. Zhao, E. Zhao, X. Qiu, S. Li, K. Li, *Strategic Planning for Energy Environ.* **2024**, *43*, 665.
[49] G. L. Soloveichik, *Annu. Rev. Chem. Biomol. Eng.* **2011**, *2*, 503.
[50] Z. Wen, J. Cao, Z. Gu, X. Xu, F. Zhang, Z. Lin, *Solid State Ionics* **2008**, *179*, 1697.
[51] M. Armand, J. M. Tarascon, *Nature* **2008**, *451*, 652.
[52] V.r. Toniazzo, *J. Power Sources* **2006**, *158*, 1124.
[53] B. Scrosati, J.r. Garche, *J. Power Sources* **2010**, *195*, 2419.
[54] J. Chen, G. Qi, K. Wang, *Energies* **2023**, *16*, 6318.
[55] H. Fu, B. Gao, Y. Qiao, Lin, Z. Liu, S. Yuan, A. Abdelkader, A. R. Kamali, *J. Energy Storage* **2024**, *86*, 111555.
[56] Y. Sun, J. Sun, J. S. Sanchez, Z. Xia, L. Xiao, R. Chen, V. Palermo, *Chem. Commun.* **2023**, *59*, 2571.
[57] C. Sole, N. E. Drewett, F. Liu, A. M. Abdelkader, I. A. Kinloch, L. J. Hardwick, *J. Electroanal. Chem.* **2015**, *753*, 35.
[58] N. Fernando, H. Kannan, F. C. Robles Hernandez, M. Ajayan, A. Meiyazhagan, A. M. Abdelkader, *J. Energy Storage* **2023**, *71*, 108015.
[59] L. Xu, W. Lv, K. Shi, S. Xiao, C. You, Y.-B. He, F. Kang, Q.-H. Yang, *Carbon* **2019**, *149*, 257.
[60] J. K. Lee, K. B. Smith, C. M. Hayner, H. H. Kung, *Chem Commun.* **2010**, *46*, 2025.
[61] Y. Joshi, A. Umasankaran, C. Klaassen, M. AlAmer, Y. L. Joo, *Electrochim. Acta* **2022**, *404*, 139753.
[62] J.-Z. Wang, C. Zhong, S.-L. Chou, H.-K. Liu, *Electrochem. Commun.* **2010**, *12*, 1467.
[63] W. Sun, R. Hu, H. Liu, M. Zeng, L. Yang, H. Wang, M. Zhu, *J. Power Sources* **2014**, *268*, 610.
[64] W. Sun, R. Hu, H. Zhang, Y. Wang, L. Yang, J. Liu, M. Zhu, *Electrochim. Acta* **2016**, *187*, 1.
[65] L. Liu, X. Li, G. Zhang, Z. Zhang, C. Fang, H. Ma, W. Luo, Z. Liu, *ACS Omega* **2019**, *4*, 18195.
[66] T. Cetinkaya, S. Ozcan, M. Uysal, M. O. Guler, H. Akbulut, *J. Power Sources* **2014**, *267*, 140.
[67] S.-H. Peng, T.-H. Chen, C.-H. Lee, H.-C. Lu, S. J. Lue, *J. Power Sources* **2020**, *471*, 228373.
[68] M. Ren, J. Zhang, J. M. Tour, *Carbon* **2018**, *139*, 880.
[69] F. Cheng, J. Zhao, W. Song, C. Li, H. Ma, J. Chen, Shen, *Inorg. Chem.* **2006**, *45*, 2038.
[70] A. Zahoor, H. S. Jang, J. S. Jeong, M. Christy, Y. J. Hwang, K. S. Nahm, *RSC Adv.* **2014**, *4*, 8973.
[71] F. Cheng, Y. Su, J. Liang, Z. Tao, J. Chen, *Chem. Mater.* **2010**, *22*, 898.
[72] J. Liu, Y. Zhao, X. Li, C. Wang, Y. Zeng, G. Yue, Q. Chen, *Nano-Micro Lett.* **2017**, *10*, 22.
[73] Y. Jiang, J. Cheng, L. Zou, X. Li, Y. Huang, L. Jia, B. Chi, J. Pu, J. Li, *ChemCatChem* **2017**, *9*, 4231.

[74] N. Feng, X. Mu, M. Zheng, C. Wang, Z. Lin, X. Zhang, Y. Shi, He, H. Zhou, *Nanotechnology* **2016**, *27*, 365402.
[75] M. D. Stoller, S. Park, Z. Yanwu, J. An, R. S. Ruoff, *Nano Lett.* **2008**, *8*, 3498.
[76] J. Yan, J. Liu, Z. Fan, T. Wei, L. Zhang, *Carbon* **2012**, *50*, 2179.
[77] D. Chen, H. Feng, J. Li, *Chem. Rev.* **2012**, *112*, 6027.
[78] A. Bello, O. O. Fashedemi, J. N. Lekitima, M. Fabiane, D. Dodoo-Arhin, K. I. Ozoemena, Y. Gogotsi, A. T. Charlie Johnson, N. Manyala, *AIP Adv.* **2013**, *3*, 082118.
[79] L. Zhang, G. Shi, *J. Phys. Chem. C* **2011**, *115*, 17206.
[80] Z. Lei, L. Lu, X. S. Zhao, *Energy Environ. Sci.* **2012**, *5*, 6391.
[81] S. R. C. Vivekchand, C. S. Rout, K. S. Subrahmanyam, A. Govindaraj, C. N. R. Rao, *J. Chem. Sci.* **2008**, *120*, 9.
[82] Y. Zhu, S. Murali, M. D. Stoller, K. J. Ganesh, W. Cai, J. Ferreira, A. Pirkle, R. M. Wallace, K. A. Cychosz, M. Thommes, D. Su, E. A. Stach, R. S. Ruoff, *Science* **2011**, *332*, 1537.
[83] A. M. Abdelkader, *J. Mater. Chem. A* **2015**, *3*, 8519.
[84] G. Yu, X. Xie, L. Pan, Z. Bao, Y. Cui, *Nano Energy* **2013**, *2*, 213.
[85] P. Liu, H. Wang, T. Yan, J. Zhang, L. Shi, D. Zhang, *J. Mater. Chem. A* **2016**, *4*, 5303.
[86] H. Yin, S. Zhao, J. Wan, H. Tang, L. Chang, L. He, H. Zhao, Y. Gao, Z. Tang, *Adv. Mater.* **2013**, *25*, 6270.
[87] Y. Liu, C. Xiang, H. Chu, S. Qiu, J. McLeod, Z. She, F. Xu, L. Sun, Y. Zou, *J. Mater. Sci. Technol.* **2020**, *37*, 135.
[88] D. Chu, F. Li, X. Song, H. Ma, L. Tan, H. Pang, X. Wang, D. Guo, B. Xiao, *J. Colloid Interface Sci.* **2020**, *568*, 130.
[89] H. M. Jeong, J. W. Lee, W. H. Shin, Y. J. Choi, H. J. Shin, J. K. Kang, J. W. Choi, *Nano Lett.* **2011**, *11*, 2472.
[90] L. Qu, Y. Liu, J. B. Baek, L. Dai, *ACS Nano* **2010**, *4*, 1321.
[91] X. Wang, X. Li, L. Zhang, Y. Yoon, K. Weber, H. Wang, J. Guo, H. Dai, *Science* **2009**, *324*, 768.
[92] L. S. Panchakarla, K. S. Subrahmanyam, S. K. Saha, A. Govindaraj, H. R. Krishnamurthy, U. V. Waghmare, C. N. R. Rao, *Adv. Mater.* **2009**, *21*, 4726.
[93] D. Geng, Y. Chen, Y. Chen, Y. Li, R. Li, X. Sun, S. Ye, S. Knights, *Energy Environmental Sci.* **2011**, *4*, 760.
[94] A. Abdelkader, D. Fray, *Nanoscale* **2017**, *9*, 14548.
[95] A. M. Abdelkader, D. J. Fray, *Nanoscale* **2017**, *9*, 14548.
[96] M. Dulal, M. R. Islam, S. Maiti, M. H. Islam, I. Ali, A. M. Abdelkader, K. S. Novoselov, S. Afroj, N. Karim, *Adv. Funct. Mater.* **2023**, *33*, 2305901.
[97] N. Karim, S. Afroj, D. Leech, A. M. Abdelkader, in *Flexible and Wearable Graphene-Based E-Textiles*, (Eds: A. Ray), John Wiley and Sons Inc, Hoboken, NJ **2021**, Ch. 2, https://doi.org/10.1002/9781119529538.ch2.
[98] S. Afroj, S. Tan, A. M. Abdelkader, K. S. Novoselov, N. Karim, *Adv. Funct. Mater.* **2020**, *30*, 2000293.
[99] A. M. Abdelkader, N. Karim, C. Vallés, S. Afroj, K. S. Novoselov, S. G. Yeates, *2D Mater.* **2017**, *4*, 035016.
[100] J. Liu, S. Bao, X. Wang, *Micromachines* **2022**, *13*, 184.
[101] F. Yavari, N. Koratkar, *J. Phys. Chem. Lett.* **2012**, *3*, 1746.
[102] A. Chakraborthy, S. Nuthalapati, A. Nag, N. Afsarimanesh, M. E. E. Alahi, M. E. Altinsoy, *Chemosensors* **2022**, *10*, 355.
[103] X. Zhang, H. Cui, Y. Gui, *Sensors* **2017**, *17*, 363.
[104] H. Bai, H. Guo, J. Wang, Y. Dong, B. Liu, Z. Xie, F. Guo, D. Chen, R. Zhang, Y. Zheng, *Sens. Actuators, B* **2021**, *337*, 129783.
[105] J. Feng, Q. Li, J. Cai, T. Yang, J. Chen, X. Hou, *Sens. Actuators, B* **2019**, *298*, 126872.
[106] M. Ferraro,., G. C. Curhan, *Am. J. Kidney Dis.* **2017**, *70*, 158.
[107] Q. Li, C. Huo, K. Yi, L. Zhou, L. Su, X. Hou, *Sens. Actuators, B* **2018**, *260*, 346.
[108] Y. J. Chen, W. H. Jian, Z. Y. Liang, W. J. Guan, W. H. Liang, R. C. Chen, C. L. Tang, T. Wang, H. R. Liang, Y. M. Li, X. Q. Liu, L. Sang, L. L. Cheng, F. Ye, S. Y. Li, N. F. Zhang, Z. Zhang, Y. Fang, J. X. He, N.-S. Zhong, J. Zheng, *Ann. Transl. Med.* **2021**, *9*, 941.
[109] G. Seo, G. Lee, M. J. Kim, S.-H. Baek, M. Choi, K. B. Ku, C.-S. Lee, S. Jun, D. Park, H. G. Kim, S.-J. Kim, J.-O. Lee, B. T. Kim, E. C. Park, S. I. Kim, *ACS Nano* **2020**, *14*, 5135.
[110] M. A. Ali, C. Hu, S. Jahan, B. Yuan, M. S. Saleh, E. Ju, S. J. Gao, R. Panat, *Adv. Mater.* **2021**, *33*, 2006647.
[111] J. Mohanraj, D. Durgalakshmi, R. A. Rakkesh, S. Balakumar, S. Rajendran, H. Karimi-Maleh, *J. Colloid Interface Sci.* **2020**, *566*, 463.
[112] D. Shahdeo, A. Roberts, N. Abbineni, S. Gandhi, in *Comprehensive Analytical Chemistry* (Ed: C. M. Hussain), Elsevier, Amsterdam, Netherlands **2020**, Ch. 8, pp. 175–199.
[113] Q. Zheng, J.-h. Lee, X. Shen, X. Chen, J.-K. Kim, *Mater. Today* **2020**, *36*, 158.
[114] S. Nuthalapati, V. Kedambaimoole, V. Shirhatti, S. Kumar, H. Takao, M. M. Nayak, K. Rajanna, *Nanotechnology* **2021**, *32*, 505506.
[115] S. Nuthalapati, V. Shirhatti, V. Kedambaimoole, N. Neella, M. M. Nayak, K. Rajanna, H. Takao, *Nanotechnology* **2020**, *31*, 035501.
[116] K. Cao, M. Wu, J. Bai, Z. Wen, J. Zhang, T. Wang, M. Peng, T. Liu, Z. Jia, Z. Liang, *Adv. Funct. Mater.* **2022**, *32*, 2202360.
[117] X. Che, M. Wu, G. Yu, C. Liu, H. Xu, B. Li, C. Li, *Chem. Eng. J.* **2022**, *433*, 133672.
[118] T.-Y. Zhang, Q. Wang, N.-Q. Deng, H.-M. Zhao, D.-Y. Wang, Z. Yang, Y. Liu, Y. Yang, T.-L. Ren, *Appl. Phys. Lett.* **2017**, *111*, 121901.
[119] L. Lu, W. Chen, *Adv. Mater.* **2010**, *22*, 3745.
[120] Y.-L. Zhang, J.-C. Li, H. Zhou, Y.-Q. Liu, D.-D. Han, H.-B. Sun, *The Innovation* **2021**, *2*, 100168.
[121] K. M. Salleh, N. A. Zainul Armir, N. S. N. Mazlan, M. Mostapha, C. Wang, S. Zakaria, in *Biodegradable Polymers, Blends and Composites* (Eds: S. Mavinkere Rangappa, J. Parameswaranpillai, S. Siengchin, M. Ramesh), Woodhead Publishing, Sawston, UK **2022**, pp. 355–388.
[122] R. Curvello, V. S. Raghuwanshi, G. Garnier, *Adv. Colloid Interface Sci.* **2019**, *267*, 47.
[123] Q. Zheng, M. Shang, X. Li, L. Jiang, L. Chen, J. Long, A. Jiao, H. Ji, Z. Jin, C. Qiu, *Food Hydrocolloids* **2024**, *146*, 109190.
[124] Y. Shi, J. Zhang, L. Pan, Y. Shi, G. Yu, *Nano Today* **2016**, *11*, 738.
[125] H. Mittal, A. Al Alili, P. Morajkar, S. M. Alhassan, *Int. J. Biol. Macromol.* **2021**, *167*, 1248.
[126] P. Song, B. Liu, C. Liang, K. Ruan, H. Qiu, Z. Ma, Y. Guo, J. Gu, *Nano-Micro Lett.* **2021**, *13*, 91.
[127] I. Ali, X. Mbianda, A. Burakov, E. Galunin, I. Burakova, E. Mkrtchyan, A. Tkachev, V. Grachev, *Environment Int.* **2019**, *127*, 160.
[128] Z.-y. Han, L.-j. Huang, H.-j. Qu, Y.-x. Wang, Z.-j. Zhang, Q.-l. Rong, Z.-q. Sang, Y. Wang, M. J. Kipper, J.-g. Tang, *J. Mater. Sci.* **2021**, *56*, 9545.
[129] H. S. Abbo, K. C. Gupta, N. G. Khaligh, S. J. J. Titinchi, *ChemBioEng Rev.* **2021**, *8*, 46.
[130] M. R. Gandhi, S. Vasudevan, A. Shibayama, M. Yamada, *ChemistrySelect* **2016**, *1*, 4358.
[131] M. Safarpour, A. Khataee, in *Nanoscale Materials in Water Purification* (Eds: S. Thomas, D. Pasquini, S.-Y. Leu, D. A. Gopakumar), Elsevier, Amsterdam, Netherlands **2019**, pp. 383–430.
[132] Y. Cao, X. Li, *Adsorption* **2014**, *20*, 713.
[133] G. Ersan, O. G. Apul, F. Perreault, T. Karanfil, *Water Res.* **2017**, *126*, 385.
[134] S. Mohan, V. Kumar, D. K. Singh, S. H. Hasan, *J. Environ. Chem. Eng.* **2017**, *5*, 2259.
[135] J. Bao, Y. Fu, Z. Bao, *Nanoscale Res. Lett.* **2013**, *8*, 486.
[136] J. Zhu, Z. Lou, Y. Liu, R. Fu, S. A. Baig, X. Xu, *RSC Adv.* **2015**, *5*, 67951.
[137] Q.-U. Ain, M. U. Farooq, M. I. Jalees, *J. Water Process Eng.* **2020**, *33*, 101044.

[138] J. R. Koduru, R. R. Karri, N. Mubarak, in *Sustainable Polymer Composites and Nanocomposites*, Springer, Cham, Switzerland **2019**, pp. 759–781.
[139] Y. Li, Q. Du, T. Liu, J. Sun, Y. Wang, S. Wu, Z. Wang, Y. Xia, L. Xia, *Carbohydr. Polym.* **2013**, *95*, 501.
[140] Z. Wu, H. Zhong, X. Yuan, H. Wang, L. Wang, X. Chen, G. Zeng, Y. Wu, *Water Res.* **2014**, *67*, 330.
[141] J. A. González, M. E. Villanueva, L. L. Piehl, G. J. Copello, *Chem. Eng. J.* **2015**, *280*, 41.
[142] N. Baig, M. S. Ihsanullah, T. A. Saleh, *J. Environm. Manag.* **2019**, *244*, 370.
[143] W. W. Anku, E. M. Kiarii, R. Sharma, G. M. Joshi, S. K. Shukla, P. Govender, in *A New Generation Material Graphene: Applications in Water Technology* (Ed: M. Naushad), Springer International Publishing, Cham, Switzerland **2019**, pp. 187–208.
[144] S. Kumar, C. Terashima, A. Fujishima, V. Krishnan, S. Pitchaimuthu, in *A New Generation Material Graphene: Applications in Water Technology* (Ed: M. Naushad), Springer International Publishing, Cham, Switzerland **2019**, pp. 413–438.
[145] H. Dong, G. Zeng, L. Tang, C. Fan, C. Zhang, X. He, Y. He, *Water Res.* **2015**, *79*, 128.
[146] F. Zhang, Y.-H. Li, J.-Y. Li, Z.-R. Tang, Y.-J. Xu, *Environm. Poll.* **2019**, *253*, 365.
[147] Y. Vasseghian, E.-N. Dragoi, F. Almomani, V. T. Le, M. Berkani, *Environm. Technol. Innovation* **2021**, *24*, 101863.
[148] M.-m. Cheng, L.-j. Huang, Y.-x. Wang, J.-g. Tang, Y. Wang, Y.-c. Zhao, G.-f. Liu, Y. Zhang, M. J. Kipper, S. R. Wickramasinghe, *Sep. Sci. Technol.* **2019**, *54*, 1079.
[149] M. Ahmed, A. Giwa, S. W. Hasan, in *Nanoscale Materials in Water Purification* (Eds: S. Thomas, D. Pasquini, S.-Y. Leu, D. A. Gopakumar), Elsevier, Amsterdam, Netherlands **2019**, pp. 735–758.
[150] V. T. Le, F. Almomani, Y. Vasseghian, J. A. Vilas-Boas, E.-N. Dragoi, *Food Chem. Toxicol.* **2021**, *148*, 111964.
[151] N. Karki, H. Tiwari, C. Tewari, A. Rana, N. Pandey, S. Basak, N. G. Sahoo, *J. Mater. Chem. B* **2020**, *8*, 8116.
[152] K. Yang, L.-j. Huang, Y.-x. Wang, Y.-c. Du, J.-g. Tang, Y. Wang, M.-m. Cheng, Y. Zhang, M. J. Kipper, L. A. Belfiore, S. R. Wickramasinghe, *New J. Chem.* **2019**, *43*, 2846.
[153] M. Fathizadeh, H. N. Tien, K. Khivantsev, J.-T. Chen, M. Yu, *J. Mater. Chem. A* **2017**, *5*, 20860.
[154] A. Khataee, M. Safarpour, M. Zarei, S. Aber, *J. Mol. Catal. A: Chem.* **2012**, *363–364*, 58.
[155] E. Mousset, Z. Wang, J. Hammaker, O. Lefebvre, *Electrochim. Acta* **2016**, *214*, 217.
[156] M. Bassyouni, M. Abdel-Aziz, M. S. Zoromba, S. Abdel-Hamid, E. Drioli, *J. Ind. Eng. Chem.* **2019**, *73*, 19.
[157] E. F. D. Januário, T. B. Vidovix, N.d.C. L. Beluci, R. M. Paixão, L. H. B. R.d. Silva, N. C. Homem, R. Bergamasco, A. M. S. Vieira, *Sci. Total Environ.* **2021**, *789*, 147957.
[158] H. Naeem, M. Ajmal, S. Muntha, J. Ambreen, M. Siddiq, *RSC Adv.* **2018**, *8*, 3599.
[159] M. Yang, C. Zhao, S. Zhang, Li, D. Hou, *Appl. Surf. Sci.* **2017**, *394*, 149.
[160] J. Xu, H. Lv, S.-T. Yang, J. Luo, *Rev. Inorg. Chem.* **2013**, *33*, 139.
[161] M.-f. Li, Y.-g. Liu, G.-m. Zeng, N. Liu, S.-b. Liu, *Chemosphere* **2019**, *226*, 360.
[162] Y. Li, L. Chen, Y. Wang, L. Zhu, *Mater. Sci. Eng., B* **2016**, *210*, 29.
[163] A. Alammar, S.-H. Park, C. J. Williams, B. Derby, G. Szekely, *J. Membr. Sci.* **2020**, *603*, 118007.
[164] N. F. D. Junaidi, N. H. Othman, N. S. Fuzil, M. S. Mat Shayuti, N. H. Alias, M. Z. Shahruddin, F. Marpani, W. J. Lau, A. F. Ismail, N. D. Aba, *Sep. Purif. Technol.* **2021**, *258*, 118000.
[165] W. Peng, H. Li, Y. Liu, S. Song, *J. Mol. Liq.* **2017**, *230*, 496.
[166] C. E. D. Cardoso, J. C. Almeida, C. B. Lopes, T. Trindade, C. Vale, E. Pereira, *Nanomaterials* **2019**, *9*, 814.
[167] X. Liu, R. Ma, X. Wang, Y. Ma, Y. Yang, L. Zhuang, S. Zhang, R. Jehan, J. Chen, X. Wang, *Environm. Pollut.* **2019**, *252*, 62.
[168] M. Liu, C. Chen, J. Hu, X. Wu, X. Wang, *J. Phys. Chem. C* **2011**, *115*, 25234.
[169] P. Zong, S. Wang, Y. Zhao, H. Wang, H. Pan, C. He, *Chem. Eng. J.* **2013**, *220*, 45.
[170] D. Cohen-Tanugi, J. C. Grossman, *Nano Lett.* **2012**, *12*, 3602.
[171] N. Song, X. Gao, Z. Ma, X. Wang, Y. Wei, C. Gao, *Desalination* **2018**, *437*, 59.
[172] Y. Li, W. Zhao, M. Weyland, S. Yuan, Y. Xia, H. Liu, M. Jian, J. Yang, C. D. Easton, C. Selomulya, X. Zhang, *Environ. Sci. Technol.* **2019**, *53*, 8314.
[173] N. Yousefi, X. Lu, M. Elimelech, N. Tufenkji, *Nat. Nanotechnol.* **2019**, *14*, 107.
[174] A. V. Meshkov, A. A. Nikitina, T. A. Aliev, V. S. Gromov, S. Chen, K. Yang, Q. Wang, K. S. Novoselov, D. V. Andreeva, E. V. Skorb, *Adv. Int. Syst.* **2024**, *6*, 2300655.
[175] H. Yang, Z. Chen, Y. Li, L. Yao, G. Wang, Q. Deng, Fu, S. Wang, *J. Water Process Eng.* **2023**, *55*, 104088.
[176] B. Zheng, G. X. Gu, *Nano-Micro Lett.* **2020**, *12*, 181.

Maryam A. Saeed is an Associate Research Scientist in the Nanotechnology and Advanced Materials Program at the Kuwait Institute for Scientific Research. She earned her Ph.D. in Nanostructures Materials from the University of Manchester where she worked on her research at the National Graphene Institute. She holds a Master's degree in Physics from Glasgow University. She currently leads a team working on graphene and 2D materials at the Kuwait Institute for Scientific Research. Her main scope of research is graphene growth and processing.

Amor M. Abdelkader is an associate professor of advanced materials at Bournemouth University and the director of the BU-NEU Joint Centre for Advanced Materials. He leads a team working on developing materials for energy and sustainability. He earned his Ph.D. in Materials Science from the University of Cambridge. Before his appointment at Bournemouth, Dr Abdelkader held several positions at the University of Cambridge, the University of Manchester, and Delft University of Technology. He has published over 100 papers in high-impact journals and contributed to over 20 patents.

Yousef Alshammari is an assistant research scientist at the Kuwait Institute for Research Center. He obtained his Ph.D., Master's, and bachelor's degrees from the University of Waikato in New Zealand. Previously, he worked as an assistant professor at the International University of Kuwait. His research interests include designing, fabricating, and characterizing metallic alloys and composites. Additionally, he is interested in the field of Biomaterials and anticorrosion alloys.

Cristina Vallés is a Lecturer in Polymer Nanocomposites at the Department of Materials (University of Manchester, UK). She leads a research group focused on the development of multifunctional polymer nanocomposites for applications in the aerospace sector and nanostructured polymer fibers for wearable electronics. Her research activity in the field of Functional Nanomaterials has been published in over 60 high-ranking, peer-reviewed international journals. She has presented her research work at more than 50 International Scientific Conferences and has two international patents accepted out of her work.

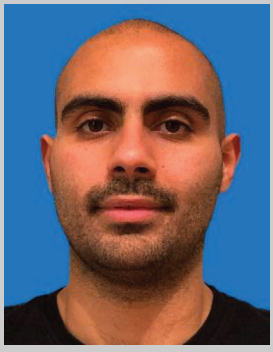

Abdullah Alkandary is a research associate in the nanotechnology and advanced materials program at the Kuwait Institute for Scientific Research. He holds a BSc in nuclear engineering from Pennsylvania State University and an MSc in materials science and engineering from Cornell University. He is a published author in energy storage nanomaterials and biocomposites, moreover, he holds five patents in the areas of fuel cells and photovoltaic sensors. His current research is concerned with mimicking lignocellulosic structures following *green chemistry*, toward the synthesis of advanced biodegradable biocompatible polymer matrix composites.